ary approximate derivations of some retarded two dielectric walls. *Physical Review A, 48,*

xperimental studies of helium Rydberg fine *ılar Physics, Comments on Modern Physics, Part*

e electromagnetic forces in quantum theory: . Micha (Eds.) *Long range Casimir forces: Theory* . 273–348). New York: Plenum Press.
uations and intermolecular interactions. *Phy-*

05). Interaction of ultracold antihydrogen with 062903.
ı problems and Pollaczek polynomials. *Journal*

V. (1999). Temperature dependence of atom– 581–2584.
g-range interactions of lithium atoms. *Physical*

& Stancil, P. C. (2003). Multichannel study of quency shift and line broadening in cold colli- A, 67, 042715.

CHAPTER 2

Advances in Coherent Population Trapping for Atomic Clocks

Vishal Shah[a] and **John Kitching**[b]

[a]*Symmetricom Technology Realization Center, 34 Tozer Road, Beverly, MA 01915, USA*
[b]*Time and Frequency Division, NIST, 325 Broadway, Boulder, CO 80305, USA*

Contents

1. Coherent Population Trapping 22
   1.1 Introduction 22
   1.2 Basic Principles 23
2. Atomic Clocks 27
   2.1 Introduction 27
   2.2 Vapor Cell Atomic Clocks 29
   2.3 Coherent Population Trapping in Atomic Clocks 30
   2.4 Stability of Vapor Cell Atomic Clocks 35
   2.5 Light Shifts 38
3. Advanced CPT Techniques 39
   3.1 Contrast Limitations due to Excited-State Hyperfine Structure 40
   3.2 Contrast Limitations due to Zeeman Substructure 42
   3.3 High-Contrast Resonances Using Four-Wave Mixing 51
   3.4 Push–Pull Laser Atomic Oscillator 52
   3.5 The CPT Maser 54
   3.6 N-Resonance 55
   3.7 Raman–Ramsey Pulsed CPT 56
   3.8 CPT in Optical Clocks 59
4. Additional Considerations 60
   4.1 Light-Shift Suppression 60
   4.2 Laser Noise Cancellation 61
   4.3 Light Sources for Coherent Population Trapping 64

Advances in Atomic, Molecular, and Optical Physics, Volume 59
ISSN 1049-250X, DOI: 10.1016/S1049-250X(10)59002-5

4.4 Dark Resonances in Thin Cells 65
4.5 The Lineshape of CPT Resonances: Narrowing Effects 65
5. Conclusions and Outlook 66
Acknowledgments 67
References 67

Abstract

We review advances in the field of coherent population trapping (CPT) over the last decade with respect to the application of this physical phenomenon to atomic frequency references. We provide an overview of both the basic phenomenon of CPT and how it has traditionally been used in atomic clocks. We then describe a number of advances made with the goal of improving the resonance contrast, decreasing its line width, and reducing light shifts that affect the long-term stability. We conclude with a discussion of how these new approaches can impact future generations of laboratory and commercial instruments.

1. COHERENT POPULATION TRAPPING

1.1 Introduction

Coherent population trapping (CPT) (Arimondo, 1996) refers to the preparation of atoms in coherent superposition states by use of multimode optical fields. This phenomenon, as investigated using hyperfine (Alzetta et al., 1976; Arimondo & Orriols, 1976) and optical (Whitley & Stroud, 1976) transitions in 1976, has led to significant advances in a variety of areas of optical and atomic physics including laser cooling (Aspect et al., 1988), nonlinear optics (Hemmer et al., 1995), precision spectroscopy (Wynands & Nagel, 1999), slow light (Schmidt et al., 1996), atomic clocks (Kitching et al., 2000; Thomas et al., 1981, 1982; Vanier et al., 1998; Zanon et al., 2005; Zanon-Willette et al., 2006), and other precision spectroscopic instrumentation (Nagel et al., 1998; Schwindt et al., 2004). The central principle that underlies the value of CPT in this diverse set of applications is the idea that certain coherent superposition states do not absorb light from the excitation field. This reduced absorption leads both to a spectroscopic signal on the light field and to a modified atom–light interaction.

The use of CPT in atomic clocks is a particularly important application that has sustained interest over three decades. Early work to use microwave CPT (Arimondo & Orriols, 1976; Orriols, 1979) in atomic beam clocks (Thomas et al., 1981, 1982) has been adapted for application to vapor cell clocks (Cyr et al., 1993; V
to microfabricated atomic clocks (
of atomic microwave clocks based
(2005). Possible future application
ered (Hong et al., 2005; Santra et a
resonance is used to directly me
The performance of the clock ther
of the CPT resonance, and most sp

This chapter reviews research
extend the phenomenon of CPT v
frequency standards. Special emp
detection schemes, and other ne
nance contrast, reduce its line wi
fields on the resonance frequenc
phenomenon of CPT and describe
been excited and detected. In Sec
atomic clocks and discuss the dif
clocks and those based on CPT. In
of the simplest CPT excitation sche
have been recently developed to
nance for use in atomic clocks. I
outstanding issues including lig
unique experimental environment
Section 5, we offer some conclus
connected with CPT may ultimat
atomic frequency references.

1.2 Basic Principles

A two-level atom illuminated by a
is perhaps the simplest spectrosco
illumination field is tuned into res
atomic levels, radiation is scattere
sion, causing fluorescence, and a
and phase of the transmitted radi
signal, combined with a measure
frequency, often gives highly pr
structure of the atom. In atoms
variety of more complex phenom
optical pumping, in which light
causes atomic population to accu
light field (see Figure 1b). Once p
stop scattering light to the extent
resonant with the light field. Such

k Resonances in Thin Cells 65
Lineshape of CPT Resonances:
owing Effects 65
ns and Outlook 66
nts 67
67

vances in the field of coherent population over the last decade with respect to the this physical phenomenon to atomic ences. We provide an overview of both the non of CPT and how it has traditionally been c clocks. We then describe a number of with the goal of improving the resonance asing its line width, and reducing light shifts long-term stability. We conclude with a ow these new approaches can impact future aboratory and commercial instruments.

ON TRAPPING

CPT) (Arimondo, 1996) refers to the pre- uperposition states by use of multimode as investigated using hyperfine (Alzetta s, 1976) and optical (Whitley & Stroud, d to significant advances in a variety of ics including laser cooling (Aspect et al., er et al., 1995), precision spectroscopy light (Schmidt et al., 1996), atomic clocks al., 1981, 1982; Vanier et al., 1998; Zanon 2006), and other precision spectroscopic 998; Schwindt et al., 2004). The central ue of CPT in this diverse set of applica- erent superposition states do not absorb This reduced absorption leads both to a ht field and to a modified atom–light

ks is a particularly important application three decades. Early work to use micro- ls, 1976; Orriols, 1979) in atomic beam 82) has been adapted for application to vapor cell clocks (Cyr et al., 1993; Vanier et al., 1998) and led most recently to microfabricated atomic clocks (Knappe et al., 2004). A previous review of atomic microwave clocks based on CPT is given in the work of Vanier (2005). Possible future application to optical clocks has also been considered (Hong et al., 2005; Santra et al., 2005). In these clock designs, the CPT resonance is used to directly measure the atomic transition frequency. The performance of the clock therefore depends intimately on the quality of the CPT resonance, and most specifically on its line width and contrast.

This chapter reviews research over the last decade to understand and extend the phenomenon of CPT with respect to its application to atomic frequency standards. Special emphasis is placed on novel excitation and detection schemes, and other new phenomena that improve the resonance contrast, reduce its line width, or minimize the effect of the light fields on the resonance frequency. In Section 1.2, we review the basic phenomenon of CPT and describe how CPT resonances have traditionally been excited and detected. In Section 2, we provide an introduction to atomic clocks and discuss the differences between conventional atomic clocks and those based on CPT. In Section 3, we consider the limitations of the simplest CPT excitation schemes and describe several schemes that have been recently developed to enhance the quality of the CPT resonance for use in atomic clocks. In Section 4, we address a number of outstanding issues including light shifts, light sources for CPT, and unique experimental environments in which CPT is observed. Finally in Section 5, we offer some conclusions and discuss how the new ideas connected with CPT may ultimately impact the development of future atomic frequency references.

1.2 Basic Principles

A two-level atom illuminated by a monochromatic electromagnetic field is perhaps the simplest spectroscopic system. When the frequency of the illumination field is tuned into resonance with the transition between the atomic levels, radiation is scattered by the atom via spontaneous emission, causing fluorescence, and a corresponding change in the intensity and phase of the transmitted radiation (see Figure 1a). The fluorescence signal, combined with a measurement of the radiation wavelength or frequency, often gives highly precise information about the internal structure of the atom. In atoms with more than two energy levels, a variety of more complex phenomena can occur. One example of this is optical pumping, in which light resonant with one optical transition causes atomic population to accumulate in a state not excited by the light field (see Figure 1b). Once pumped into this third state, the atoms stop scattering light to the extent that the third state is stable and not resonant with the light field. Such a state is referred to as a dark state.

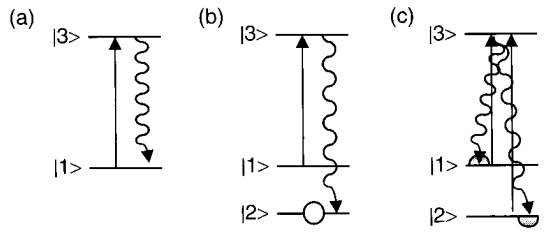

Figure 1 Optically excited transitions in atoms. (a) Simple excitation of a two-level atom. (b) Optical pumping in a three-level atom. Level |2> is an incoherent dark state. (c) Bichromatic excitation of a three-level atom. A superposition of levels |1> and |2> is a coherent dark state

CPT is a phenomenon that occurs in atoms with more than two energy levels excited by coherent, multimode optical fields. Under the right conditions, atoms are optically pumped into a superposition of two of the levels that does not scatter light from the multimode field (see Figure 1c). This coherent dark state has an electromagnetic moment that oscillates at one of the beat frequencies of the multimode field. Its excitation can be thought of as a nonlinear process: a nonlinear resonator (the atom) is driven with a force with two spectral components (the light), and through the nonlinearity, an oscillation at the sum or difference of the two driving frequencies is established. The phase of this oscillation, with respect to the phase of the driving fields, is such that no energy is absorbed.

CPT between hyperfine atomic levels was first observed experimentally in a seminal paper by Alzetta et al. (1976), in which a light field from a multi-longitudinal-mode dye laser was sent into a vapor cell containing saturated Na and a buffer gas. The laser mode spacing had a harmonic near the frequency of the ground-state hyperfine splitting of Na. A longitudinal magnetic field gradient was applied to the cell, and the fluorescence from the cell was measured as a function of longitudinal position. Dark lines were observed in the fluorescence at locations where the magnetic field had shifted magnetically sensitive hyperfine levels into resonance with a mode spacing harmonic. Data from Alzetta et al. (1976) are shown in Figure 2.

The observations were explained theoretically by use of a density matrix analysis, in which the excited-state population, and hence the fluorescence rate, in the three-level system was calculated as a function of the relative detuning of a pair of resonant optical fields (Arimondo & Orriols, 1976; Gray et al., 1978; Whitley & Stroud, 1976;). The dark line in the fluorescence was identified as resulting from (destructive) interference of absorption pathways in the coherently excited atomic system.

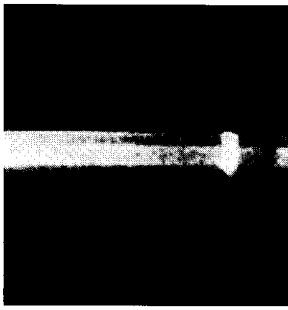

Figure 2 Data showing the fluorescer
multimode optical field. A magnetic fie
light propagation. Three dark lines are
Reprinted figure with permission from
Italiana de Fisica

A similar phenomenon on the Z
was reported earlier by Bell and
given by Arimondo (1996).

A key aspect of this phen
at microwave frequencies can be
being present at the location of t
excited entirely by two-photon
and have a line width determin
addition, the presence of the co
itoring the fluorescence (or abso

CPT can also be understood as
and optical pumping. In the thre
couples two long-lived states (de
single upper level (denoted |3>)
and the optical field is denoted

$$E(t) = \varepsilon_1 e^{-i(}$$

where ε_i, ω_i, and ϕ_i are the (comp
the ith field component, respect
positions of states |1> and |2>
distinct ways:

$$|NC\rangle =$$

$$|C\rangle =$$

Here

$$c_i = \frac{}{\sqrt{|\mu_1 \varepsilon_1|^2}}$$

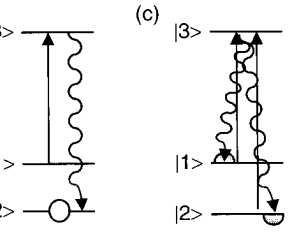

atoms. (a) Simple excitation of a two-level
l atom. Level |2> is an incoherent dark state.
atom. A superposition of levels |1> and |2>

rs in atoms with more than two energy
mode optical fields. Under the right
umped into a superposition of two of
light from the multimode field (see
e has an electromagnetic moment that
ncies of the multimode field. Its excita-
ear process: a nonlinear resonator (the
vo spectral components (the light), and
tion at the sum or difference of the two
d. The phase of this oscillation, with
ing fields, is such that no energy is

levels was first observed experimen-
et al. (1976), in which a light field from
er was sent into a vapor cell containing
ne laser mode spacing had a harmonic
state hyperfine splitting of Na. A long-
vas applied to the cell, and the fluores-
as a function of longitudinal position.
fluorescence at locations where the
etically sensitive hyperfine levels into
armonic. Data from Alzetta et al. (1976)

ned theoretically by use of a density
cited-state population, and hence the
el system was calculated as a function
of resonant optical fields (Arimondo &
nitley & Stroud, 1976;). The dark line in
s resulting from (destructive) interfer-
the coherently excited atomic system.

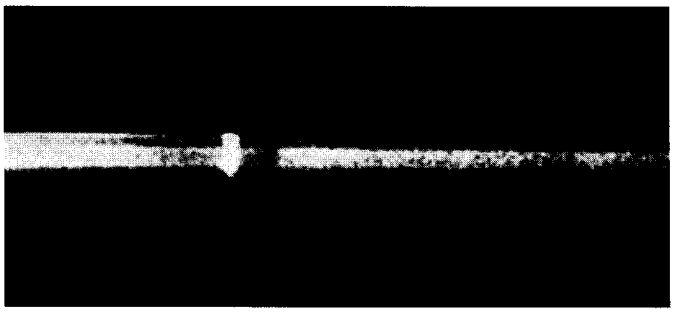

Figure 2 Data showing the fluorescence from a Na vapor cell under illumination by a multimode optical field. A magnetic field is applied with a gradient along the axis of the light propagation. Three dark lines are observed in the fluorescence spectrum. Reprinted figure with permission from Alzetta et al. (1976); © 1976 of the Società Italiana de Fisica

A similar phenomenon on the Zeeman rather than hyperfine coherences was reported earlier by Bell and Bloom (1961), and a review of CPT is given by Arimondo (1996).

A key aspect of this phenomenon is that coherences in atoms at microwave frequencies can be excited even with no microwave fields being present at the location of the atoms. The hyperfine coherences are excited entirely by two-photon processes involving only optical fields and have a line width determined by the hyperfine relaxation rate. In addition, the presence of the coherence can be detected easily by monitoring the fluorescence (or absorption) by the atomic sample.

CPT can also be understood as a combination of quantum interference and optical pumping. In the three-level model, a bichromatic optical field couples two long-lived states (denoted |1> and |2> in the Figure 1c) to a single upper level (denoted |3>). The energy of the ith level is denoted E_i and the optical field is denoted

$$E(t) = \varepsilon_1 e^{-i(\omega_1 t+\phi_1)} + \varepsilon_2 e^{-i(\omega_2 t+\phi_2)}, \tag{1}$$

where ε_i, ω_i, and ϕ_i are the (complex) amplitude, frequency, and phase of the ith field component, respectively. We may write orthogonal superpositions of states |1> and |2> that interact with the optical field in distinct ways:

$$\begin{aligned} |NC\rangle &= c_2|1\rangle - c_1|2\rangle \\ |C\rangle &= c_1^*|1\rangle + c_2^*|2\rangle. \end{aligned} \tag{2}$$

Here

$$c_i = \frac{\mu_i \varepsilon_i}{\sqrt{|\mu_1\varepsilon_1|^2 + |\mu_2\varepsilon_2|^2}} e^{i[(E_i/h)t+\phi_i]}, \tag{3}$$

and μ_i is the electric dipole moment between state $|i\rangle$ and state $|3\rangle$. It can be shown that when the two-photon resonance condition, $\omega_1-\omega_2 = (E_1-E_2)/\hbar$, is fulfilled, the transition amplitude from the state $|NC\rangle$ to the excited state $|3\rangle$ is zero. The $|NC\rangle$ state is therefore a dark (or "non-coupled") state, because no light is scattered when the resonance condition is fulfilled. The suppression of the transition amplitude can be interpreted as a result of quantum interference between transitions from states $|1\rangle$ and $|2\rangle$ to state $|3\rangle$ under the influence of the exciting optical field (Alzetta et al., 1976; Arimondo, 1996; Lounis & Cohen-Tannoudji, 1992).

An atomic sample initially in a thermal state will develop coherences when illuminated with a bichromatic field satisfying the resonance condition. This can be thought of as an optical pumping effect: atoms in the "bright" (or "coupled") state $|C\rangle$ will be excited to level $|3\rangle$ and will eventually fall into the dark state, where they no longer interact with the optical field. Population therefore builds up in the dark state and the absorption of the optical field (and fluorescence from the atomic sample) is reduced. As a function of two-photon detuning, we therefore observe a resonance in the absorption/fluorescence signal.

In the data shown in Figure 2, CPT resonances are observed in the fluorescence spectrum of a cell subjected to a magnetic field gradient. CPT resonances are also frequently observed in the transmission spectrum of light passing through an atomic sample in the presence of a uniform magnetic field, as shown in Figure 3. In this case the frequency difference between the two excitation fields is scanned over the hyperfine transition frequency and a spectrum containing a number of absorption resonances can be observed as a function of difference frequency, corresponding to transitions between different pairs of Zeeman-split hyperfine levels. In the case of circularly polarized light and a longitudinal magnetic field, only transitions between Zeeman levels with $\Delta m_F = 0$ are observed, resulting in a spectrum consisting of $2I$ lines for an atom with nuclear spin I. For atoms with half-integer nuclear spin, the central line (corresponding to $m_F = 0 \rightarrow m_F = 0$) occurs at a frequency close to the

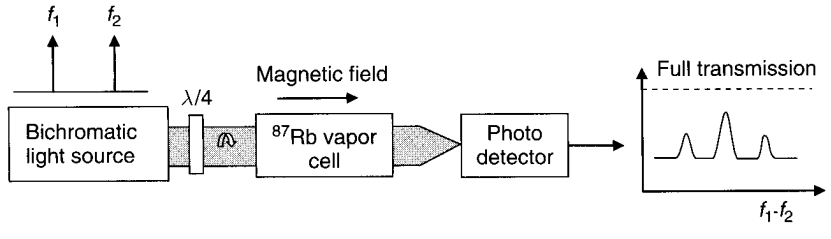

Figure 3 Coherent population trapping resonance spectrum observed in the transmitted light through a vapor cell subject to a uniform magnetic field

zero-field hyperfine splitting
from the central line by even
where γ is the gyromagnetic
nuclear spin have more Zeem
of correspondingly more lines
transverse component, the CP
way between the $\Delta m_F = 0$ lin
Transitions with $\Delta m_F = 2$ can
description of the CPT spectr
Knappe (2001).

The bichromatic light nee
generated in a number of wa
direct modulation of the inje
1993) and phase-locking of tw
tion is simpler to implement b
consisting of more than two fr
difficult to control. The use of
plicated locking electronics b
and allows a high degree of fr
tion and amplitude of these co

2. ATOMIC CLOCKS

2.1 Introduction

Most atomic clocks are based
which have a single valence el
is relatively simple, and long
tion, narrow transition line wi
In addition to charge, both the
all alkali atoms have spin ang
moment. Microwave frequenc
tions between atomic states th
nuclear and electron magnetic
the order of 1–10 GHz, when t
by Planck's constant h.

With some notable excepti
2005b), microwave atomic clo
magnetically insensitive m_F =
folds. Clocks based on states
careful simultaneous measure
prevent variations in this par
clock frequency. While this lat

zero-field hyperfine splitting of the atom. The other lines are separated from the central line by even multiples of the Larmor frequency $f_L = \gamma B_0$, where γ is the gyromagnetic ratio of the atoms. Atoms with higher nuclear spin have more Zeeman levels, and the CPT spectrum consists of correspondingly more lines. If the magnetic field is rotated so it has a transverse component, the CPT spectrum displays additional lines halfway between the $\Delta m_F = 0$ lines corresponding to $\Delta m_F = 1$ transitions. Transitions with $\Delta m_F = 2$ can also be excited. For a more complete description of the CPT spectrum, see Wynands and Nagel (1999) and Knappe (2001).

The bichromatic light needed to excite the CPT resonance can be generated in a number of ways. The two most common methods are direct modulation of the injection current of a laser diode (Cyr et al., 1993) and phase-locking of two lasers (Nagel et al., 1998). Direct modulation is simpler to implement but results in an optical spectrum typically consisting of more than two frequencies with spectral amplitudes that are difficult to control. The use of injection-locked lasers requires more complicated locking electronics but results in only two optical frequencies and allows a high degree of freedom in controlling the relative polarization and amplitude of these components.

2. ATOMIC CLOCKS

2.1 Introduction

Most atomic clocks are based on alkali atoms (in particular H, Rb, Cs), which have a single valence electron. In these atoms, the energy spectrum is relatively simple, and long-lived ground states result in slow relaxation, narrow transition line widths, and correspondingly high precision. In addition to charge, both the atomic nucleus and the valence electron of all alkali atoms have spin angular momentum, and therefore a magnetic moment. Microwave frequency references are based on hyperfine transitions between atomic states that differ in the relative orientation of the nuclear and electron magnetic moments. This difference in energies is on the order of 1–10 GHz, when translated into frequency units by dividing by Planck's constant h.

With some notable exceptions (Post et al., 2003; Taichenachev et al., 2005b), microwave atomic clocks are based on transitions between the magnetically insensitive $m_F = 0$ substates of different hyperfine manifolds. Clocks based on states for which $m_F \neq 0$ (but $\Delta m_F = 0$) require a careful simultaneous measurement of the local magnetic field in order to prevent variations in this parameter from resulting in variations of the clock frequency. While this latter approach is not altogether prohibitive, it

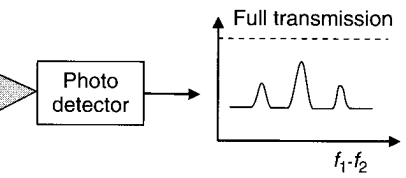

onance spectrum observed in the
ct to a uniform magnetic field

adds significant complications to the operation of the device and has not found widespread popularity. On the other hand, optical clocks based on fermionic alkaline earth atoms have a small linear Zeeman shift that is effectively and routinely removed with appropriate interrogation techniques (Akatsuka et al., 2008).

The measurement of transitions between these atomic states can be accomplished in several ways. Perhaps the simplest measurement method is the passive excitation method, where an oscillating magnetic field is applied to the atoms at a frequency corresponding to the energy difference. When the frequency of the applied field is close to the frequency of the atomic transition, an oscillating moment (coherence) is excited in the atom. Most frequently, magnetic dipole moments are excited. This coherence allows energy to be transferred from the field (atom) to the atom (field), and changes the internal state of the atom.

Because this energy transfer is a resonant effect, the internal state of the atom can be monitored to determine when the frequency of the applied field corresponds to the energy splitting of the atomic states being coupled. A typical atomic frequency reference can be thought of as a series of steps. The atoms are first prepared in one specific atomic state (by magnetic state selection, optical pumping, or some other means). The oscillating magnetic field, generated by a "local oscillator" (LO), is then applied, causing some fraction of the atoms to change their state; this fraction depends on whether the frequency of the oscillating field is on-resonance with the atoms. Finally the number of atoms in the final state (or the initial state) is detected, again by optical or magnetic means. Because of the resonant nature of the interaction, the number of atoms in the final state depends on the difference between the frequencies of the oscillating field and the atomic transition, and a measurement of this quantity can therefore be used in a feedback loop to lock the frequency of the oscillating field to the atomic transition frequency. The output of the clock is simply the frequency of the locked LO. The operation of a basic passive atomic frequency reference is shown in Figure 4.

Atomic clocks based on alkali atoms can be divided into four main categories. Fountain clocks (Clairon et al., 1991; Kasevich et al., 1989; Zacharias, 1953), the most accurate atomic clocks at present, are large devices that often take up the better part of an entire room and require several hundred watts of power. There exist perhaps 10 such instruments worldwide and each typically takes several person-years to construct and evaluate. Hydrogen masers (Gordon et al., 1954), highly stable over long time periods, are about the size of a large filing cabinet. Cs beam clocks (Essen & Parry, 1955; Ramsey, 1950), based on beams of alkali atoms in a vacuum, are also highly accurate and are manufactured in rack-mounted enclosures. Vapor cell atomic clocks are based on atoms confined in a cell with a buffer gas (Arditi, 1958; Carver, 1957; Dicke, 1953) or wall coating

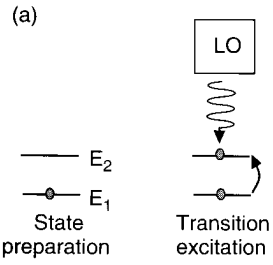

Figure 4 (a) The operation of a pass in three steps. First the atom is prepa the local oscillator is then applied, ca The number of atoms in the final stat of the local oscillator can be determi

(Goldenberg et al., 1961; Robin vapor cell clocks are manufac These clocks are typically stabl are intrinsically accurate (with pact vapor cell atomic clocks, industry, can be held in the about 10^{-11}.

2.2 Vapor Cell Atomic Clocks

A schematic of a traditional Rb Audoin, 1992) is shown in Figu is a vapor cell that contains t density of buffer gas. The vap cavity into which a microwave

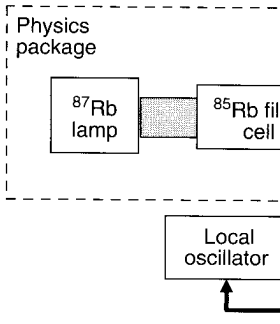

Figure 5 Schematic of the major co reference

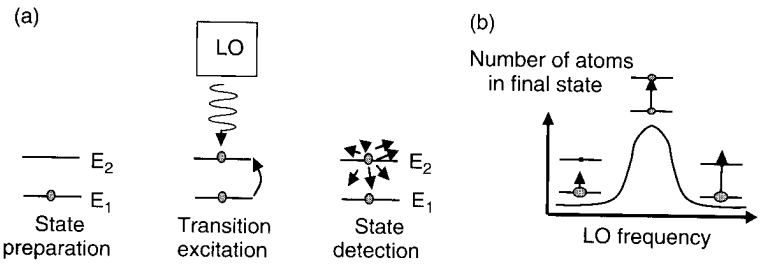

Figure 4 (a) The operation of a passive atomic frequency reference typically proceeds in three steps. First the atom is prepared in some energy state, E_1. The frequency from the local oscillator is then applied, causing transitions to another state with energy E_2. The number of atoms in the final state is detected. (b) With this method, the frequency of the local oscillator can be determined with respect to the atomic transition

(Goldenberg et al., 1961; Robinson et al., 1958). The highest-performance vapor cell clocks are manufactured for installation on GPS satellites. These clocks are typically stable to 10^{-13} or better over long periods but are intrinsically accurate (without calibration) only to about 10^{-9}. Compact vapor cell atomic clocks, developed for the telecommunications industry, can be held in the palm of one hand and are stable to about 10^{-11}.

2.2 Vapor Cell Atomic Clocks

A schematic of a traditional Rb vapor cell frequency reference (Vanier & Audoin, 1992) is shown in Figure 5. The heart of the frequency reference is a vapor cell that contains the Rb vapor, along with an appropriate density of buffer gas. The vapor cell is contained within a microwave cavity into which a microwave field is injected. The microwave field is

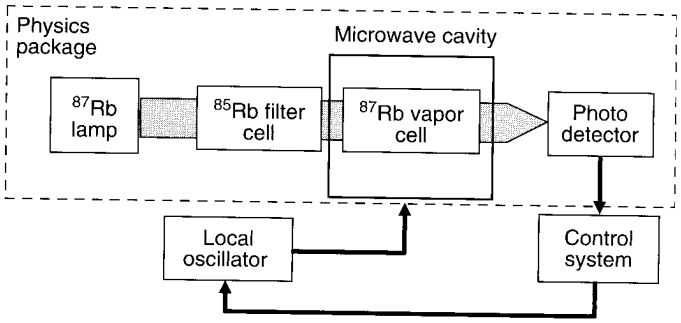

Figure 5 Schematic of the major components of a traditional vapor cell frequency reference

generated by a LO, which is usually based on an electromechanical resonator (such as a quartz crystal resonator). Because the LO is an electromechanical device, it is typically rather unstable over long periods; the atoms therefore provide a stable reference frequency to which the LO can be locked. The atoms in the cell are illuminated by light generated by a Rb lamp. The Rb lamp is a second glass cell, containing Rb, through which an RF discharge is excited.

Light from the lamp, with appropriate filtering, serves to prepare the atoms in the reference cell in one of the two hyperfine ground states via optical pumping. Because of this optical pumping, the atoms in the reference cell become less absorbing than they would in a thermal distribution. As the frequency of the RF field is tuned to near the atomic resonance, the population distribution in the reference cell changes again as the hyperfine populations are returned closer to their thermal distribution. This in turn increases the atomic absorption, and the increased absorption can be detected by monitoring the optical power transmitted through the cell with a photodiode. The transmitted optical power, as a function of microwave frequency, therefore becomes the "signal" to which the LO is locked.

2.3 Coherent Population Trapping in Atomic Clocks

CPT was first used in atomic clocks in the early 1980s (Ezekiel et al., 1983; Hemmer et al., 1983a, 1984; Thomas et al., 1981, 1982). In these experiments, modulated dye lasers were used to excite microwave transitions in a Na beam atomic clock. In effect, CPT zones replaced the microwave cavities employed in a conventional beam clock based on Ramsey's method of separated oscillatory fields: in the first CPT zone the atomic coherence was created, and in the second, its phase was compared to that of the drive signal. Although initial investigations focused on the hyperfine transition in Na at 1.77 GHz, the use of optical fields to excite the coherence opened the door to the possibility of exciting atomic coherences in frequency bands far beyond the gigahertz range. A Ramsey zone separation of 15 cm led to a resonance line width of 2.6 kHz (see Figure 6), and a corresponding frequency instability of 8×10^{-10} at 1 second was measured, as shown in Figure 7. A subsequent experiment using a Cs atomic beam, excited by a modulated diode laser, demonstrated resonance widths of 1 kHz and a projected instability of 6×10^{-11} at 1 second (Hemmer et al., 1993). The signal-to-noise ratio was about 10 times worse than that predicted by photon shot noise and was limited by frequency noise on the diode laser being translated into intensity noise on the measured atomic fluorescence. The conversion of FM to AM noise continues to be an important source of instability in the current generation of laser-pumped atomic clocks (Camparo & Coffer, 1999; Kitching et al., 2000).

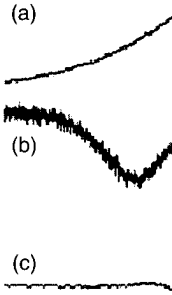

Figure 6 (a) and (b) Rabi fringes f
laser. (c) Raman–Ramsey fringes w
permission from Thomas et al. (19

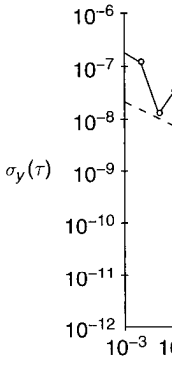

Figure 7 Allan deviation of a frequ
of CPT resonances in a Na atomic
Hemmer et al. (1983b); © 1983 of t

These early experiments no
CPT in atomic frequency refere
to both the short-term frequ
frequency instability common
include the FM–AM noise cor
shot noise, and instability aris
Sources of frequency inst

ually based on an electromechanical
al resonator). Because the LO is an
ally rather unstable over long periods;
e reference frequency to which the LO
are illuminated by light generated by
nd glass cell, containing Rb, through

opriate filtering, serves to prepare the
f the two hyperfine ground states via
optical pumping, the atoms in the
ng than they would in a thermal dis-
RF field is tuned to near the atomic
ion in the reference cell changes again
urned closer to their thermal distribu-
tomic absorption, and the increased
nitoring the optical power transmitted
e. The transmitted optical power, as a
, therefore becomes the "signal" to

g in Atomic Clocks

in the early 1980s (Ezekiel et al., 1983;
as et al., 1981, 1982). In these experi-
used to excite microwave transitions in
, CPT zones replaced the microwave
nal beam clock based on Ramsey's
elds: in the first CPT zone the atomic
econd, its phase was compared to that
nvestigations focused on the hyperfine
of optical fields to excite the coherence
of exciting atomic coherences in fre-
ertz range. A Ramsey zone separation
idth of 2.6 kHz (see Figure 6), and a
of 8×10^{-10} at 1 second was measured,
t experiment using a Cs atomic beam,
er, demonstrated resonance widths of
6×10^{-11} at 1 second (Hemmer et al.,
s about 10 times worse than that pre-
vas limited by frequency noise on the
tensity noise on the measured atomic
M to AM noise continues to be an
ne current generation of laser-pumped
999; Kitching et al., 2000).

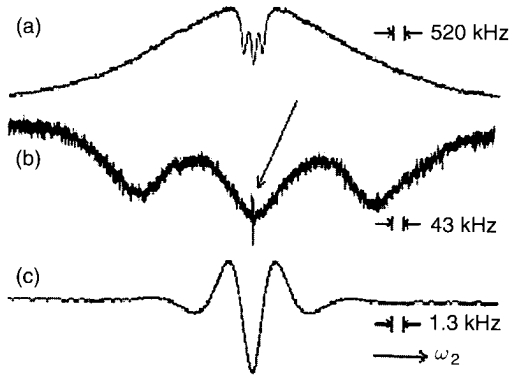

Figure 6 (a) and (b) Rabi fringes from a Na atomic beam excited by a modulated dye laser. (c) Raman–Ramsey fringes with a width of 2.6 kHz. Reprinted figure with permission from Thomas et al. (1982); © 1982 of the American Physical Society

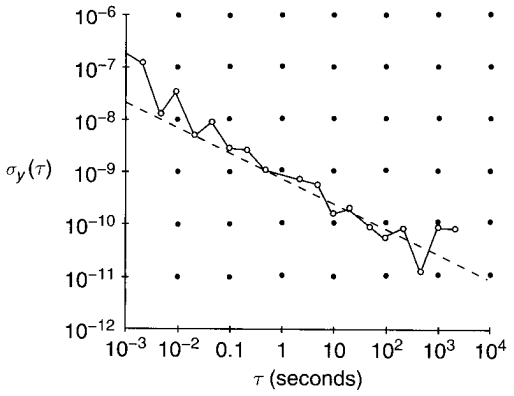

Figure 7 Allan deviation of a frequency reference based on Raman–Ramsey excitation of CPT resonances in a Na atomic beam. Reprinted figure with permission from Hemmer et al. (1983b); © 1983 of the Optical Society of America

These early experiments not only demonstrated the viability of the use of CPT in atomic frequency references but also identified the major limitations to both the short-term frequency stability and the accuracy. Sources of frequency instability common to many types of CPT frequency references include the FM–AM noise conversion mentioned above, atom and photon shot noise, and instability arising from the light shift (Hemmer et al., 1989). Sources of frequency instability associated specifically with the

Raman–Ramsey scheme include misalignment of the beams from a copropagating configuration, birefringence, and polarization differences between the beams and changes in the optical path length (Hemmer et al., 1986).

As mentioned above, semiconductor lasers have been used for CPT excitation in atomic beam clocks (Hemmer et al., 1993). The advantages of semiconductor lasers over dye lasers in this type of experiment are clear: smaller size and simpler operation. In addition, it is possible to modulate the optical field output of the laser by directly modulating the injection current. Resonances of width 1 kHz were obtained in a ^{133}Cs beam by use of an edge-emitting AlGaAs diode laser modulated at 4.6 GHz. The two coherent first-order sidebands created the 9.2-GHz frequency difference needed to excite the Raman–Ramsey fringes.

In 1993, Cyr, Tetu, and Breton described a method for exciting and detecting CPT resonances in an alkali vapor cell by use of a single diode laser (Cyr et al., 1993). The details of the experiment are shown in Figure 8. The injection current of the laser was modulated near the sixth subharmonic (1.139 GHz) of the ^{87}Rb hyperfine frequency (6.835 GHz), creating sidebands on the optical carrier, several of which are separated by approximately the atomic resonance frequency. When one of these sideband pairs was tuned to be in optical resonance with the atomic transitions, and their

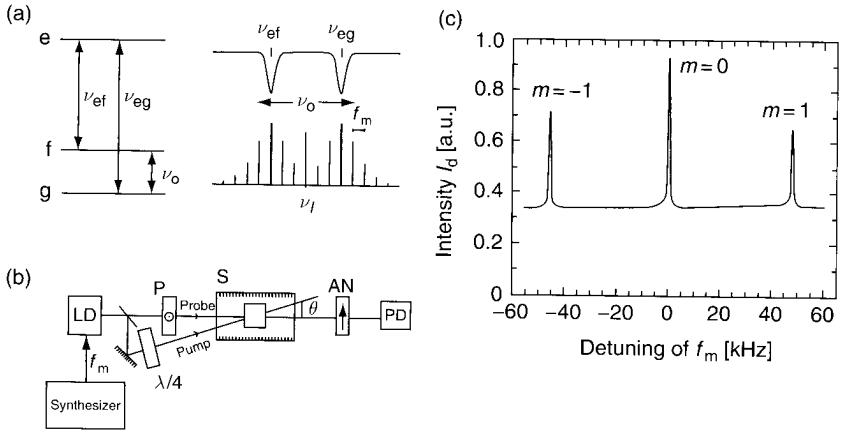

Figure 8 Excitation of CPT resonances in an alkali vapor cell with a modulated diode laser. (a) The atomic energy level spectrum and optical frequency spectrum of the modulated diode laser. The CPT resonance is excited when the frequency splitting, $\nu_0 = nf_m$, between two components of the diode laser optical spectrum is equal to the atomic ground-state hyperfine splitting, ν_{eg}-ν_{ef}. (b) Experimental setup. LD, laser diode; P, polarizer; S, solenoid; AN, polarization analyzer; PD, photodetector; $\lambda/4$, quarter-wave plate. (c) The photodetector signal as a function of the detuning of the laser modulation frequency from the sixth subharmonic of the atomic resonance frequency. Reprinted figure with permission from Cyr et al. (1993); © 1993 IEEE

difference frequency (determined by the modulation frequency) made equal to the microwave transition, a microwave coherence was excited in the atoms. This coherence was detected by monitoring the polarization rotation of a probe beam derived from the same laser (Figure 8c).

This idea is particularly noteworthy in the context of miniaturized frequency references, because all components used in the experiment are small. The use of a vapor cell lends itself well to miniaturization compared to previous CPT experiments based on atomic beams because much smaller cell sizes can be used to achieve a given short-term frequency stability, due to the presence of the buffer gas. Some time later it was demonstrated that a single laser beam could also be used, allowing for even further simplification of the experimental setup (Levi et al., 1997).

Since then, there has been considerable study of CPT-excited vapor cell frequency references. The noise processes in these instruments have been identified (Kitching et al., 2000) and short-term instabilities as low as $1.3 \times 10^{-12}/\sqrt{\tau}$ have been demonstrated in large-scale systems (Zhu & Cutler, 2000). Vapor cell CPT atomic clocks have been investigated in some detail theoretically (Vanier et al., 1998, 2003a,c,d) and experimentally (Godone et al., 2002d; Knappe et al., 2001, 2002; Levi et al., 2000; Merimaa et al., 2003; Stahler et al., 2002). They have also been compared both theoretically (Vanier, 2001b) and experimentally (Lutwak et al., 2002) to conventional optically pumped vapor cell references with the conclusion that the short-term frequency stability of CPT-based instruments should be comparable to or better than conventional ones. A review of atomic clocks based on CPT is given in the work of Vanier (2005).

In 2001, a compact physics package for CPT frequency reference was demonstrated by Kitching et al. (2001a,b). This device had a volume of about $14\,\text{cm}^3$, and the short-term stability of this device was $1.3\times10^{-10}/\sqrt{\tau}$. A photograph of the device is shown in Figure 9a, and the CPT resonance and Allan deviation are shown in Figure 9b and c, respectively. Similar work was being explored simultaneously (Delany et al., 2001; Vanier, 2001a), connected with the ultimate development of compact, commercial CPT clocks (Deng, 2008; Vanier et al., 2005). These early efforts to use CPT to miniaturize atomic frequency standards used glass-blown vapor cells with a diameter of several millimeters or more. The cells were assembled as discrete components with a laser, optics, and photodetector to form the functioning physics package.

Complete miniaturized CPT frequency references for use in a commercial setting have also been demonstrated (Deng, 2008; Vanier et al., 2004, 2005). This work demonstrated integration of a compact CPT physics package with a low-power LO and compact control electronics.

The opportunities for atomic clock miniaturization afforded by the use of CPT led to some significant developments related to use of

ıment of the beams from a copro-
l polarization differences between
h length (Hemmer et al., 1986).
lasers have been used for CPT
er et al., 1993). The advantages of
this type of experiment are clear:
ddition, it is possible to modulate
directly modulating the injection
e obtained in a ^{133}Cs beam by use
r modulated at 4.6 GHz. The two
the 9.2-GHz frequency difference
inges.
ribed a method for exciting and
apor cell by use of a single diode
experiment are shown in Figure 8.
odulated near the sixth subharmo-
e frequency (6.835 GHz), creating
of which are separated by approxi-
When one of these sideband pairs
th the atomic transitions, and their

c)

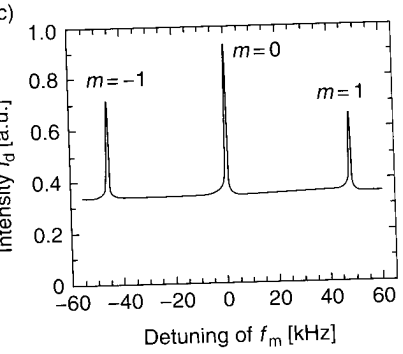

n alkali vapor cell with a modulated diode
and optical frequency spectrum of the
is excited when the frequency splitting,
ode laser optical spectrum is equal to the
ν_{ef}. (b) Experimental setup. LD, laser diode;
nalyzer; PD, photodetector; $\lambda/4$, quarter-
a function of the detuning of the laser
rmonic of the atomic resonance frequency.
et al. (1993); © 1993 IEEE

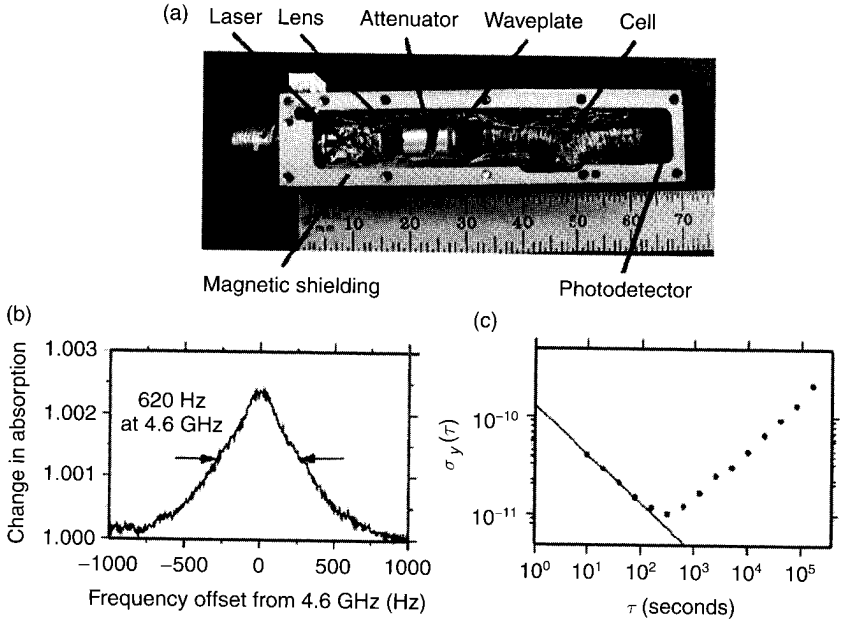

Figure 9 A miniaturized physics package for a CPT frequency reference. (a) Photograph of the instrument with major components identified. (b) CPT resonance and (c) fractional frequency instability (Allan deviation) as a function of integration period. Reprinted figure with permission from Kitching et al. (2001b)

micromachining processes in atomic clocks. A preliminary analysis suggested that CPT clocks based on millimeter-scale vapor cells could achieve short-term frequency instabilities of a few parts in 10^{11} at 1 second of integration (Kitching et al., 2002). While the stability was expected to be worse than that of their larger counterparts, it was recognized that these micromachined or "chip-scale" atomic clocks could serve an important role in providing precise timing for portable, battery-operated instruments. Because of the small size, the power required to maintain the cell at its operating temperature could be drastically reduced. When combined with similar improvements in power resulting from the use of a laser, rather than a lamp, as the light source, operation with small batteries could be envisioned. A review of chip-scale atomic frequency references can be found in the work of Knappe (2007).

Because CPT played an important role in many of these new micromachined clock designs, considerable research was carried out to improve and optimize CPT techniques specifically for this new development.

2.4 Stability of Vapor Ce

The stability of an atomic
deviation. The Allan devia
oped to quantify the fluctu
measure of the frequency i
ing a measurement of its f
For passive atomic clocks,
nant noise source, the Alla

where Q is the Q-factor o
period, S/N is the measure
and ξ is a constant of orde
sured. The frequency insta
line width, or relaxation ra
the signal strength.

In a conventional optica
quency reference, the optic
field is tuned away from r
atoms are repumped into a
(see Figure 10a). The OMD
and its transmission contra

The CPT resonance, show
the frequency difference be
transmission increases on r
The resonance can be chara
trast, denoted by W and C
quantity $B << 1$. This last co
length are such that the cell i
to the center of the optical r
characteristic of a single at

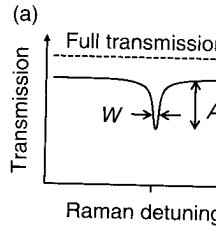

Figure 10 (a) Parameterization of
(b) Parameterization of CPT reson

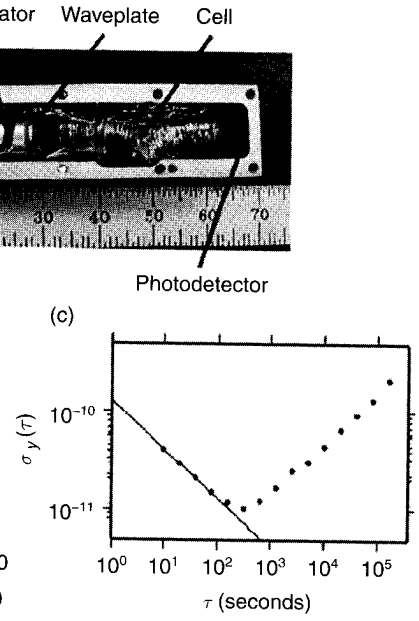

or a CPT frequency reference.
r components identified. (b) CPT resonance
n deviation) as a function of integration
om Kitching et al. (2001b)

ic clocks. A preliminary analysis
on millimeter-scale vapor cells
instabilities of a few parts in 10^{11} at
et al., 2002). While the stability
of their larger counterparts, it was
ned or "chip-scale" atomic clocks
oviding precise timing for portable,
use of the small size, the power
s operating temperature could be
ed with similar improvements in
ser, rather than a lamp, as the light
s could be envisioned. A review of
ces can be found in the work of

t role in many of these new micro-
ble research was carried out to
niques specifically for this new

2.4 Stability of Vapor Cell Atomic Clocks

The stability of an atomic clock is most often characterized by its Allan deviation. The Allan deviation (Allan, 1966; Barnes et al., 1971), developed to quantify the fluctuations of nonstationary random variables, is a measure of the frequency instability of the clock obtained after integrating a measurement of its frequency for a period τ and is denoted $\sigma_y(\tau)$. For passive atomic clocks, in which white frequency noise is the dominant noise source, the Allan deviation is given by

$$\sigma_y(\tau) = \frac{\xi}{Q(S/N)\sqrt{\tau}}, \tag{4}$$

where Q is the Q-factor of the atomic resonance, τ is the integration period, S/N is the measurement signal-to-noise ratio (in units of $\sqrt{\text{Hz}}$), and ξ is a constant of order unity related to how the resonance is measured. The frequency instability is hence proportional to the resonance line width, or relaxation rate, of the atoms and inversely proportional to the signal strength.

In a conventional optical-microwave double-resonance (OMDR) frequency reference, the optical transmission is high when the microwave field is tuned away from resonance and decreases on resonance as the atoms are repumped into an equilibrium state by the microwave field (see Figure 10a). The OMDR resonance is characterized by its width W and its transmission contrast A/B, according to Figure 10a.

The CPT resonance, shown in Figure 10b, has low transmission when the frequency difference between the optical fields is off resonance; the transmission increases on resonance when the dark state is populated. The resonance can be characterized by its width and its absorption contrast, denoted by W and $C_A = A/B$ in Figure 10b in the limit that the quantity $B << 1$. This last condition occurs when the cell temperature and length are such that the cell is optically thin for a weak optical field tuned to the center of the optical resonance. It implies that the quantity C_A is a characteristic of a single atom and the way it is excited and does not

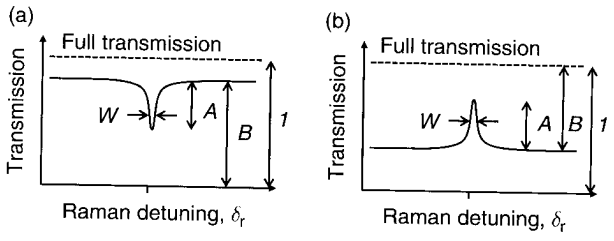

Figure 10 (a) Parameterization of conventional OMDR resonance. (b) Parameterization of CPT resonance. See text for explanation

depend on the atom density, the longitudinal location within the cell, or the effects of propagation of light through the (possibly optically thick) atomic sample.

The width of the resonance, W, is determined by relaxation processes associated with the hyperfine coherence. There are many such processes, but the ones that dominate in vapor cell atomic clocks are collisions of alkali atoms with the cell walls, collisions with buffer gas atoms, collisions with other alkali atoms, optical power broadening due to the presence of the optical field, and the relative phase stability of the excitation optical fields. This width can be minimized through the correct choice of buffer gas pressure and optical intensity. An analysis of these effects under some assumptions can be found in the work of Kitching et al. (2002).

Considering still optically thin vapor cells, we may associate the signal S in Equation (4) with the change in optical power as the modulation frequency is moved from off the CPT resonance to on resonance. The fractional (off-resonance) absorption B can be written as

$$B = \left(1 - e^{-n\sigma_0 L}\right) \approx n\sigma_0 L, \tag{5}$$

where n is the density of atoms, σ_0 is the (unpolarized) optical absorption cross section, and L is the length of the cell. The signal S can therefore be written

$$S = AP_{\text{in}} = C_{\text{A}} n\sigma_0 L P_{\text{in}}, \tag{6}$$

where P_{in} is the optical power incident on the cell. We therefore see that the signal is proportional to the column density of atoms, the incident optical power, and the absorption contrast. The typical absorption contrast for a CPT resonance is in the range of 0.1–10%; the physical effects that limit this contrast are discussed below.

As the cell temperature is increased and the optically thick regime is approached, the assumption $B \ll 1$ above breaks down. In this regime, propagation effects must be considered, and propagation-induced narrowing of the resonance and modification of the contrast occurs (Godone et al., 2002d). Experimentally, it has been found that for centimeter-scale cells, the optimal cell temperature is that for which the optical absorption (away from the CPT resonance) is approximately 0.5 (Knappe et al., 2002). At lower atomic densities, the signal is reduced due to the dependence described in Equation (6) (because very few atoms contribute toward the signal), while at higher densities, the strong optical absorption by the atomic sample attenuates the signal. While a more complete treatment of propagation effects may uncover ways to improve the clock performance at high optical densities, these remain unclear at present. Ultimately, increasing the atomic density will lead to increased hyperfine relaxation due to alkali–alkali spin-exchange or spin-destruction collisions, and any

improvements gained by the higher atom number may be offset by collision-induced broadening of the resonance line width.

The noise on the signal comes from a number of sources. Of these, photon shot noise and atom shot noise (spin projection noise) are the most fundamental. In most cases the photon shot noise is larger than the atom shot noise for measurements of hyperfine resonances; the power spectral density function of this (optical power) noise is given by (Yariv, 1997)

$$S_{\Delta P} \equiv N^2 = 2h\nu(1-B)P_{\text{in}} \approx 2h\nu(1-n\sigma_0 L)P_{\text{in}}, \tag{7}$$

with the last approximation again relying on the assumption that $B << 1$. Additional noise sources include (a) AM noise on the laser, (b) FM laser noise, converted to AM noise by the atomic absorption profile (Camparo & Coffer, 1999), and (c) noise in the detection electronics. Often it is possible to reduce these additional sources of noise to a level close to the photon shot noise through the use of feedback techniques or intrinsically low-noise lasers.

The signal-to-noise ratio can be expressed in terms of the CPT resonance parameters above as

$$\frac{S}{N} = C_A n\sigma_0 L\sqrt{\frac{(1-n\sigma_0 L)P_{\text{in}}}{2h\nu}}. \tag{8}$$

Expressed in this way, the signal-to-noise ratio is proportional to the absorption contrast and the square root of the input power, but has a somewhat complicated dependence on the alkali atom density and cell length. To simplify this problem, the signal-to-noise ratio can be expressed instead in terms of the transmission contrast $C_T = A/(1-B)$ and the output power $P_{\text{out}} = (1-B)\,P_{\text{in}}$:

$$\frac{S}{N} = C_T\sqrt{\frac{P_{\text{out}}}{2h\nu}}. \tag{9}$$

In this expression, all of the effects of the alkali density are contained within the parameters P_{out} and C_T, which can be measured experimentally in a direct manner. We see therefore that the characterization of the CPT resonance in terms of the absorption contrast C_A allows for a density-independent measure of the CPT resonance parameters, while the characterization in terms of the transmission contrast C_T allows for a simple evaluation of the signal-to-noise ratio and clock stability. Both measures of the CPT resonance contrast are used in the literature, depending on the context of the discussion.

We therefore find that there are three major routes to improving the short-term stability of the atomic clock: narrowing the resonance line width, increasing the resonance contrast, and reducing the noise. In the sections below, we describe a number of improvements and

modifications to the conventional CPT excitation scheme that result in some combination of reduced line width and increased signal contrast. These methods have been developed mostly within the last 10 years and represent a significant enhancement of the understanding of CPT, as applied to atomic frequency references.

2.5 Light Shifts

Shifts in the atomic energy levels due to the presence of optical fields, known as AC Stark shifts or light shifts, are a major source of long-term instability for atomic clocks (Arditi & Carver, 1961; Kastler, 1963; Vanier & Audoin, 1992). The use of CPT provides some additional complications, but also opportunities with respect to the light shift, compared to conventional clocks based on OMDR.

The light shift of a two-level atom illuminated by a monochromatic optical field is (Cohen-Tannoudji et al., 1992)

$$\delta_L = \frac{1}{4}\frac{\Omega^2\Delta}{(\Gamma/2)^2+\Delta^2}, \tag{10}$$

where Ω is the Rabi frequency of the optical field–atom interaction, Δ is the detuning of the optical field from the atomic resonance, and Γ is the radiative decay rate of the atom. The shift is therefore proportional to the intensity of the optical field and traces a dispersive profile as a function of detuning from the atomic resonance. For the light intensities typically used in conventional OMDR clocks, the magnitude of the shift is on the order of a few parts in 10^9 (Arditi & Carver, 1961), making it a significant contribution to the instability of this type of clock at the level of 10^{-11} for 1% changes in the light intensity.

In a system exhibiting CPT, the interplay between the coherence of the atoms and the bichromatic nature of the light field leads to changes in the properties of the light shift. The most dramatic of these changes is the complete elimination of the light shift on Raman resonance for a perfect three-level system illuminated by a light field in which the two spectral components of the CPT field have equal Rabi frequencies. This elimination is a consequence of the fact that a perfect coherent dark state does not interact dissipatively with the light field and hence does not experience a Stark shift. For unequal intensities, the Stark shift has been calculated to be equal to (Arimondo, 1996; Kelley et al., 1994; Vanier et al., 1998)

$$\delta_L = \frac{1}{4}\frac{\Delta}{(\Gamma/2)^2+\Delta^2}\left(\Omega_1^2-\Omega_2^2\right), \tag{11}$$

where Ω_1 and Ω_2 are the Rabi frequencies associated with the two spectral components. The fact that the light shift can in principle be eliminated is

of high interest to the app
source of long-term instabi
we will see below, the cor
levels, Doppler broadeni
systems limit the extent t
be accomplished in practi

Measurements of the l
Nagel et al. (1999) and Zh
light shift of approximatel
roughly optimal buffer g
obtained in conventional
roughly linear in the CPT
gas pressures.

3. ADVANCED CPT TI

In its simplest form, CPT c
levels by use of a single p
these assumptions, and
optically pumped into a c
100%. Optically pumping
ent dark state even under
rate to be much greater tha
in significant power broad
reduces the resonance Q-fa
clock operation is chosen s
equal to the ground-state
about 50% of the atoms ar

Laboratory CPT exper
atoms, especially when t
The presence of additiona
with the efficient excitati
reduce the contrast of
reduced contrast results i
unwanted energy levels i
lineshape (Post, 2003) an
adversely affect the ato
dependent frequency shif
are further amplified if a l
for CPT excitation. Over t
interrogation techniques h
ing some of these effects a
atomic clock performance.

CPT excitation scheme that result in
width and increased signal contrast.
d mostly within the last 10 years and
nt of the understanding of CPT, as
ces.

ue to the presence of optical fields,
ifts, are a major source of long-term
Carver, 1961; Kastler, 1963; Vanier &
ides some additional complications,
to the light shift, compared to con-

m illuminated by a monochromatic
al., 1992)

$$\frac{\Omega^2\Delta}{/2)^2+\Delta^2}, \tag{10}$$

e optical field–atom interaction, Δ is
n the atomic resonance, and Γ is the
shift is therefore proportional to the
s a dispersive profile as a function of
e. For the light intensities typically
the magnitude of the shift is on the
Carver, 1961), making it a significant
type of clock at the level of 10^{-11} for

interplay between the coherence of
of the light field leads to changes in
most dramatic of these changes is
nt shift on Raman resonance for a
d by a light field in which the two
d have equal Rabi frequencies. This
act that a perfect coherent dark state
the light field and hence does not
ual intensities, the Stark shift has
ndo, 1996; Kelley et al., 1994; Vanier

$$\frac{}{\Delta^2}\left(\Omega_1^2-\Omega_2^2\right), \tag{11}$$

cies associated with the two spectral
ift can in principle be eliminated is

of high interest to the application of CPT to atomic clocks, as this major source of long-term instability can potentially be eliminated. However, as we will see below, the complications associated with the multiplicity of levels, Doppler broadening, and other effects present in real atomic systems limit the extent to which the cancellation of the light shift can be accomplished in practice.

Measurements of the light shift in CPT systems were described by Nagel et al. (1999) and Zhu and Cutler (2000), and a magnitude of the light shift of approximately $10^{-7}/(\mathrm{mW/cm^2})$ was obtained for cells with a roughly optimal buffer gas pressure. This shift is comparable to that obtained in conventional OMDR systems. The shift was found to be roughly linear in the CPT intensity and was smaller for higher buffer gas pressures.

3. ADVANCED CPT TECHNIQUES

In its simplest form, CPT can be excited in atoms with only three energy levels by use of a single pair of coherent light fields. In principle under these assumptions, and with sufficient light intensity, atoms can be optically pumped into a coherent dark state with an efficiency of nearly 100%. Optically pumping a very large fraction of the atoms into a coherent dark state even under ideal conditions requires the optical pumping rate to be much greater than the ground-state relaxation rate. This results in significant power broadening and is not ideal for clock operation, as it reduces the resonance Q-factor. Typically, the optical intensity for normal clock operation is chosen such that the power broadening rate is roughly equal to the ground-state relaxation rate; under these circumstances, about 50% of the atoms are optically pumped into the coherent state.

Laboratory CPT experiments are usually carried out with alkali atoms, especially when the application is microwave atomic clocks. The presence of additional energy levels in these atoms can interfere with the efficient excitation of the coherent dark states and thereby reduce the contrast of CPT resonances. As discussed above, the reduced contrast results in higher instability for the clock. In addition, unwanted energy levels introduce asymmetries in the CPT resonance lineshape (Post, 2003) and produce AC Stark shifts, both of which adversely affect the atomic clock performance by producing time-dependent frequency shifts of the clock output. Some of these effects are further amplified if a light field with more than two modes is used for CPT excitation. Over the last several years, a number of advanced interrogation techniques have been developed with the goal of mitigating some of these effects and thereby improving various aspects of the atomic clock performance.

The following section is not an exhaustive review of the literature but seeks instead to provide an overview and the general direction of many of the approaches.

3.1 Contrast Limitations due to Excited-State Hyperfine Structure

The existence of a magnetic moment in the nucleus of all stable alkali atoms creates hyperfine structure not only the in the ground $S_{1/2}$ state but also in the P states to which the S state is coupled by the optical fields. The frequency separation of these excited-state hyperfine states (~500 MHz) is often smaller than the homogeneous broadening of the optical transition resulting from the buffer gas (2 GHz for a buffer gas pressure of 10 kPa). As a result, the optical fields used to excite the CPT resonance typically couple to several excited-state hyperfine levels simultaneously. While some of the transitions help optically prepare atoms in the coherent dark state, other transitions can simultaneously depopulate the dark state through incoherent optical pumping of atoms out of the dark state. For example, in ^{87}Rb, the $F' = 0$ and $F' = 3$ excited-state hyperfine levels in the $^5P_{3/2}$ state are coupled to only one of the two ground states, due to single-photon selection rules. As a result, a coherence between the two ground states cannot be generated by these levels via CPT, but single-photon transitions out of the CPT state to these levels are allowed (Nagel et al., 2000).

In addition to incoherent optical pumping out of the dark state, another important destructive mechanism occurs when multiple Lambda systems are formed between a common pair of ground states and different excited states. As described in the Equation (2), the phase of the dark state is governed by the complex optical Rabi frequencies that depend on both the phase of the optical fields and the coupling coefficients between the light and atomic energy levels. When multiple Lambda systems are excited between a common pair of ground states, the existence of an overall dark state in the system is not guaranteed and depends on the relative phase between the dark states of the individual Lambda systems. If the individual dark states are out of phase, then the strength of the overall CPT resonance can be reduced or even eliminated completely in the case of perfect destructive interference (Nagel et al., 2000; Stahler et al., 2002).

Consider, for example, transitions that are excited on the D1 and the D2 line of ^{87}Rb between $m_F = 0$ ground states and the excited states by use of circularly polarized light fields exciting $\sigma+$ transitions (see level diagram in Figure 11a). In addition, we assume that the buffer gas pressure in the cell is high enough that the broadening of the optical transitions is larger than the excited hyperfine splitting. On the D1 line, there are two Lambda systems and no single-photon transitions. The two Lambda systems are

$$|F = 1, m_F = 0 > \rightarrow |F' = 1, m_F = 1 > \leftarrow |F = 2, m_F = 0 > ,$$

and

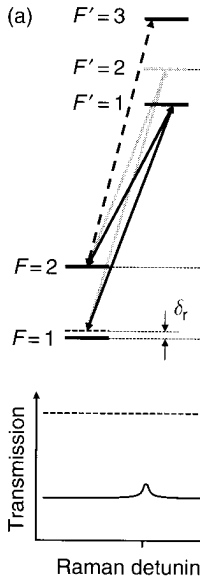

Figure 11 Simplified energy leve
transitions. The gray lines show th
show the additional transitions du
structure. The solid lines indicate
single-photon transition

$$|F = 1, m_F = 0 > \rightarrow |F$$

The transition amplitudes ar
phase and therefore add con

On the D2 transition, the s
However, due to the differen
the two dark states are qu
destruction of the CPT reso
phase factor on the D2 ^{87}Rb
state for $F = 1 \rightarrow F' = 2 \leftarrow F =$
$\rightarrow F' = 1 \leftarrow F = 2$ Lambda sy
hand, on the D1 line, the da
both Lambda systems.

In addition, on the D2 lin
depopulates the dark state:

$$|F = 2, m_F =$$

The combined influence of
CPT resonance on the D2 tra
the D1 transition.

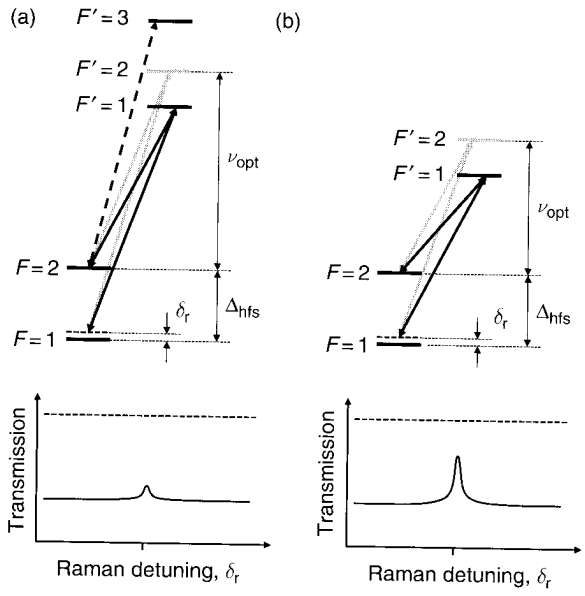

Figure 11 Simplified energy level diagram of ^{87}Rb, showing the (a) D2 and (b) D1 transitions. The gray lines show the original three-level CPT model, while the dark lines show the additional transitions due to the presence of the excited-state hyperfine structure. The solid lines indicate CPT transitions, while the dashed line indicates a single-photon transition

$$|F = 1, m_F = 0 > \rightarrow |F' = 2, m_F = 1 > \leftarrow |F = 2, m_F = 0 > .$$

The transition amplitudes are such that the individual dark states are in phase and therefore add constructively (Stahler et al., 2002).

On the D2 transition, the same two Lambda systems are again excited. However, due to the different Clebsch–Gordon coefficients, the phases of the two dark states are quite misaligned, which results in a partial destruction of the CPT resonance. For example, apart from a constant phase factor on the D2 ^{87}Rb line on the $m_F = 0$ ground states, the dark state for $F = 1 \rightarrow F' = 2 \leftarrow F = 2$ is $|NC\rangle = \frac{1}{\sqrt{2}}(|1\rangle + |2\rangle)$, and for the $F = 1 \rightarrow F' = 1 \leftarrow F = 2$ Lambda system, $|NC\rangle = \frac{1}{\sqrt{26}}(5|1\rangle + |2\rangle)$. On the other hand, on the D1 line, the dark state is given by $|NC\rangle = \frac{1}{\sqrt{2}}(|1\rangle + |2\rangle)$ for both Lambda systems.

In addition, on the D2 line there is one single-photon transition that depopulates the dark state:

$$|F = 2, m_F = 0 > \rightarrow |F' = 3, m_F = 1 > .$$

The combined influence of these two effects is that the strength of the CPT resonance on the D2 transition is significantly smaller than that on the D1 transition.

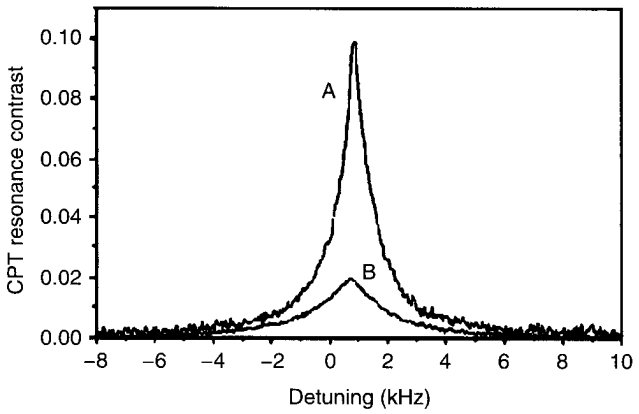

Figure 12 Comparison of CPT resonances excited using light resonant with the D1 (Trace A) and D2 (Trace B) optical transitions in ^{85}Rb. An improvement in the absorption contrast by a factor of ~10 is obtained by use of the D1 resonance. The line width of the D1-excited resonance is also narrower. Reprinted figure with permission from Stahler et al. (2002); © 2002 of the Optical Society of America

The influence of additional energy levels on CPT resonances becomes clearly evident when CPT resonances using D1 and D2 transitions are compared by use of the atomic vapor cell (Zhu, 2002). It is found experimentally that CPT resonances excited by use of the D1 transition are almost an order of magnitude stronger than those seen by use of the D2 transition (Lutwak et al., 2003; Stahler et al., 2002). A comparison of CPT resonances obtained using D1 and D2 excitation, but otherwise under similar conditions, is shown in Figure 12. The discrepancy between the strengths of the CPT resonances on the D1 and D2 transitions is in contrast with microwave resonances seen in conventional optically pumped clocks, in which efficient optical pumping can be achieved by use of both D1 and D2 transitions. The reason CPT resonances are so sensitive to excitation pathways is that CPT resonances rely equally on both optical pumping and quantum interference. This is contrasted with conventional microwave resonances that rely only on optical pumping.

3.2 Contrast Limitations due to Zeeman Substructure

The multiplicity of Zeeman levels present in the ground states of alkali atoms is another primary limitation to the signal strength. In the presence of a small magnetic field, the ground-state hyperfine levels are Zeeman split into $(2F + 1)$ magnetic ground states. In atomic clocks, a small magnetic field is typically applied to separate the various ground

states so that the magnetic
uniquely interrogated with
sitive transitions. However
spaced $m_F \neq 0$ states also in
In thermal equilibrium, at
netic sublevels with roughl
In atomic clocks, the optim
is generally weak enough
redistribution of atomic po
levels. The useable CPT res
generated by atoms that a
states with $m_F \neq 0$ contribut
tity B in Figure 10b). The a
roughly the ratio of the nu
number of ground states, u
is weak enough that it do
populations.

Another issue that is frec
the "trap state" (Renzoni &

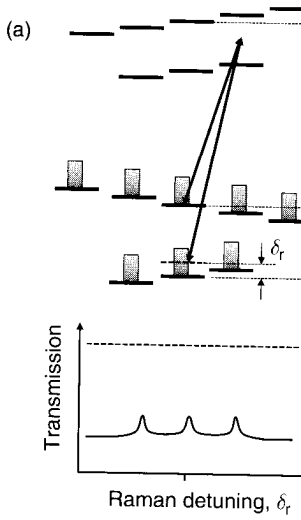

Figure 13 (a) Reduction of the CP
state Zeeman structure. An even d
state sublevels implies that only a
magnetically-insensitive $m_F = 0 \rightarrow$
(population indicated by the dark b
which atoms are pumped by the o

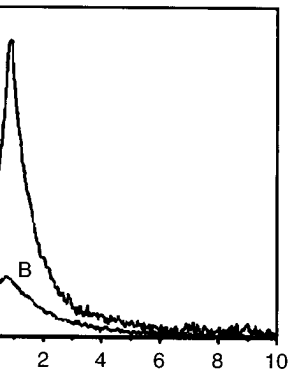

xcited using light resonant with the D1
in ^{85}Rb. An improvement in the
ned by use of the D1 resonance. The line
rower. Reprinted figure with permission
al Society of America

evels on CPT resonances becomes
using D1 and D2 transitions are
or cell (Zhu, 2002). It is found
xcited by use of the D1 transition
nger than those seen by use of the
hler et al., 2002). A comparison of
nd D2 excitation, but otherwise
in Figure 12. The discrepancy
onances on the D1 and D2 transi-
resonances seen in conventional
efficient optical pumping can
D2 transitions. The reason CPT
tion pathways is that CPT reso-
mping and quantum interference.
microwave resonances that rely

man Substructure

sent in the ground states of alkali
o the signal strength. In the pre-
ground-state hyperfine levels are
ground states. In atomic clocks, a
ed to separate the various ground

states so that the magnetically insensitive $m_F = 0$ ground states can be uniquely interrogated without interference from the magnetically sensitive transitions. However, the presence of the unwanted but closely spaced $m_F \neq 0$ states also influences the strength of the CPT resonance. In thermal equilibrium, atoms populate all of the ground-state magnetic sublevels with roughly equal probability, as shown in Figure 13a. In atomic clocks, the optimized light intensity used for CPT excitation is generally weak enough that it causes some, but not significant, redistribution of atomic population between the various magnetic sublevels. The useable CPT resonance signal (quantity A in Figure 10b) is generated by atoms that are in the $m_F = 0$ states, but many atoms in states with $m_F \neq 0$ contribute to absorption of the incident light (quantity B in Figure 10b). The absorption contrast is therefore reduced by roughly the ratio of the number of $m_F = 0$ ground states to the total number of ground states, under the assumption that the light intensity is weak enough that it does not significantly redistribute the level populations.

Another issue that is frequently discussed is optical pumping loss to the "trap state" (Renzoni & Arimondo, 1998; Vanier et al., 2003b). When

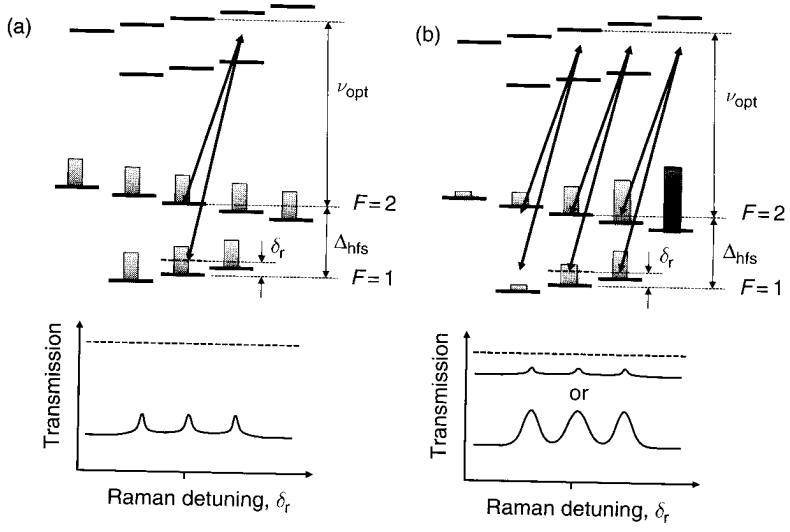

Figure 13 (a) Reduction of the CPT resonance contrast due to the presence of ground-state Zeeman structure. An even distribution of atoms among the Zeeman ground-state sublevels implies that only a small fraction of atoms contribute to the magnetically-insensitive $m_F = 0 \rightarrow m_F = 0$ transition. (b) Effects of the "trap" state (population indicated by the dark bar), which does not form a CPT resonance and into which atoms are pumped by the optical fields

circularly polarized light resonant with the D1 transition is used to excite CPT resonance, for example, a significant fraction of the population can be pumped to the magnetic end states ($F = I + 1/2$, $m_F = \pm F$). As seen in Figure 13b, the magnetic end state is an incoherent state, which is dark due to selection rules which prohibit excitation by circularly polarized light fields ($\sigma+$ transitions in this case). Atoms can therefore be "trapped" in this end state (or even in other states, depending on the laser polarization) and stop interacting with the light fields. Because the optical configuration described above is used in current generation of microwave CPT clocks, the problem of the trap state has received significant attention from the research community. This configuration in which a Lambda system is excited in the presence of an incoherent dark state is often referred to as an open Lambda system.

The atoms that are trapped or lost to the end state contribute neither to the CPT resonance signal nor to the optical absorption. They are simply invisible to the incident light fields. To compensate for this loss of atomic population, alkali density can be increased, but this also increases relaxation through alkali density dependent decoherence mechanisms such as spin exchange (Happer, 1972), which increases the line width of the CPT resonance. There have been a number of solutions that have been proposed to depopulate the end state. Some of the approaches are outlined below.

3.2.1 Depopulation Pumping Using π-Polarized Light

This idea involves use of an additional linearly polarized laser light resonant with the $F = I + 1/2$ ground state and the $F' = I + 1/2$ excited state (Kazakov et al., 2005b). The linearly-polarized light travels in a direction perpendicular to the applied magnetic field such that it excites π-transitions ($\Delta m_F = 0$). This secondary light field is used to depopulate the end state but does not depopulate the atomic population in the $F = I + 1/2$, $m_F = 0$ ground because of selection rules that prohibit such a transition.

While this technique works well in theory, there are several difficulties associated with using it in a practical device. Besides the technical difficulties arising from the use of separate laser beams traveling in perpendicular directions, this technique requires selective excitation of the $F = I + 1/2$ ground state by use of the $F' = I + 1/2$ excited state. This limits the amount of buffer gas that can be used in the vapor cell to approximately below 1 kPa in Rb and Cs such that the levels in the excited state can be clearly resolved. This technique therefore presents difficulties for use with smaller cells, which typically use higher buffer gas pressures to avoid broadening of the hyperfine transition due to wall collisions. In addition, the low buffer gas pressure r laser drift and laser freque

3.2.2 Excitation with Orth

Another approach that population in the unused the CPT resonance by use This technique addresses levels and the population pumping. A linear light fi simplest example of $\sigma+$ excited by a combination Figure 14. The $\sigma+$ and σ systems on the $m_F = 0$ stat no end states that are dark simply using linearly pola between $m_F = 0$ levels doe individual dark states exc

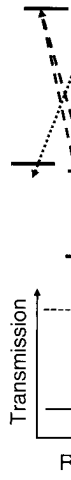

Figure 14 Excitation of CPT res fields. Destructive interference c the modulation in each polarizat $\sigma+$ polarization that excite CPT with $\sigma-$ polarization. Dotted line

collisions. In addition, the narrow optical line width resulting from the low buffer gas pressure requires tighter restrictions on the amount of laser drift and laser frequency noise that can be tolerated.

3.2.2 Excitation with Orthogonal σ-Polarized Light Fields

Another approach that has been proposed to reduce the atomic population in the unused Zeeman levels is simultaneous excitation of the CPT resonance by use of a combination of $\sigma+$ and $\sigma-$ light fields. This technique addresses both the thermal population in all Zeeman levels and the population build-up in the trap state due to optical pumping. A linear light field traveling along the magnetic field is the simplest example of $\sigma+$ and $\sigma-$ light fields. The transitions that are excited by a combination of $\sigma+$ and $\sigma-$ light fields are shown in Figure 14. The $\sigma+$ and $\sigma-$ light fields independently excite Lambda systems on the $m_F = 0$ states. As can be seen from the figure, there are no end states that are dark in this optical configuration. Unfortunately, simply using linearly polarized light to excite a closed Lambda system between $m_F = 0$ levels does not work. The reason for this is that the individual dark states excited by the $\sigma+$ and the $\sigma-$ light are out of

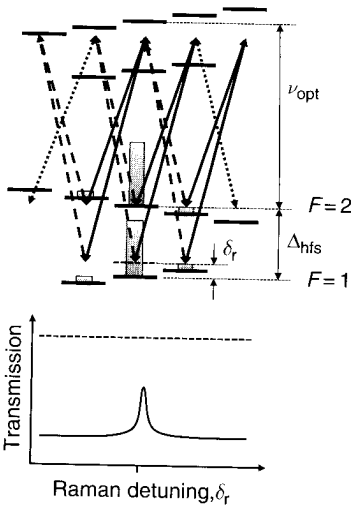

Figure 14 Excitation of CPT resonances by use of a combination of $\sigma+$ and $\sigma-$ light fields. Destructive interference can be avoided by independently adjusting the phase of the modulation in each polarization component. Solid lines indicate optical fields with $\sigma+$ polarization that excite CPT transitions, while dashed lines indicate optical fields with $\sigma-$ polarization. Dotted lines indicate depopulation pumping of "trap" states

phase. In other words, the atoms that appear dark to the $\sigma+$ polarization appear bright to the $\sigma-$ polarization, and vice versa. The result of this destructive interference is that the overall CPT resonance is not observed.

One solution to this problem is to introduce time delay between $\sigma+$ and the $\sigma-$ light fields such that the individual dark states constructively add together in phase. This principle has been successfully demonstrated in two ways. Jau et al. (2004a), Taichenachev et al. (2004b), and Kargapoltsev et al. (2004) have proposed splitting the light fields into two parts with orthogonal polarization and recombining the fields after introducing a relative path delay between the $\sigma+$ and $\sigma-$ components. The relative path difference of half a microwave wavelength (ground-state hyperfine splitting) shifts the phase of the dark state such that the resonances constructively interfere. This path length difference can be introduced by use of polarization filtering in a copropagating geometry or by reflecting the light back through the cell. A significant gain in the CPT contrast was reported by Jau et al. (2004a).

The difficulty in using additional optics in splitting and recombining the light field after introducing the path delay led to development of another similar approach (Shah et al., 2006b). In this approach two separate lasers were used to avoid the difficulty in splitting and recombining the light fields. Each of the two independent lasers had opposite circular polarizations, and they independently excited CPT resonance on the $m_F = 0$ ground states. The lasers were modulated by use of the same microwave source, and an electronic microwave phase shifter was inserted into the RF path to one laser to shift the relative phase of the microwave modulation on the two lasers by π. This technique works well and can also be implemented in a miniature package; however, the use of two separate lasers adds some complexity to the overall implementation and to the control system in particular. Another strategy is to generate a coherence on the $m_F = 0 \rightarrow m_F = 0$ transition using one polarization and measure the resonant change in birefringence with a weak optical field with an orthogonal polarization (Zhu, 2003).

3.2.3 CPT Excitation on $\Delta m_F = 2$ Transitions

A third approach that has been proposed involves the direct use of linearly polarized light and excitation of CPT resonance between $m_F = +1$ and $m_F = -1$ (Taichenachev et al., 2005b). This scheme, often referred to as "lin // lin" since two optical fields with parallel linear polarization are used, is by far the simplest way of exciting a closed Lambda transition by use of a combination of $\sigma+$ and $\sigma-$ light fields. The transitions that are excited are shown in Figure 15. The relative phase between the dark states excited between $m_F = +1 \rightarrow m_F = -1$ and $m_F = -1 \rightarrow m_F = +1$ is no

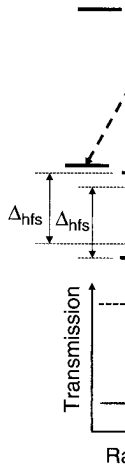

Figure 15 Excitation of CPT reson
levels

longer of concern, because
independent sets of ground s

In this scheme, the transi
magnetic field. Because of t
each of the two hyperfine le
field sensitivity for each of the
transitions. In ^{87}Rb for examp
over 300 kHz in 50 μT magne
between the states $|F = 2, m_F$
few hundred hertz because c
dependence. In addition, the
negative for one transition (
positive for the other ($|F = 2,$
when the resonance is excited
neously, the linear dependen
the resonance vanishes. The p
produces only a broadening
(2005a) have proposed using
nance by applying a magneti
the individual pairs of ground
the center to which an LO ca

The main perceived drawb
to be effective only in ^{87}Rb (
3/2) atoms but not in ^{133}Cs

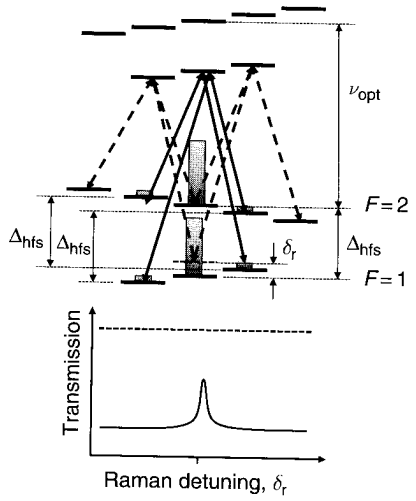

Figure 15 Excitation of CPT resonance on $\Delta m_F = 2$ transitions between hyperfine levels

longer of concern, because the dark states are excited between two independent sets of ground states.

In this scheme, the transitions have an interesting dependence on magnetic field. Because of the slightly different g-factors for states in each of the two hyperfine levels, there is a small first-order magnetic field sensitivity for each of the $m_F = +1 \rightarrow m_F = -1$ and $m_F = -1 \rightarrow m_F = +1$ transitions. In ^{87}Rb for example, individual $m_F = \pm 1$ states are shifted by over 300 kHz in 50 μT magnetic field. However, the difference frequency between the states $|F = 2, m_F = +1\rangle$ and $|F = 2, m_F = -1\rangle$ shifts by only a few hundred hertz because of their much smaller linear magnetic field dependence. In addition, the sign of this residual linear sensitivity is negative for one transition ($|F = 2, m_F = +1\rangle \leftrightarrow |F = 2, m_F = -1\rangle$) and positive for the other ($|F = 2, m_F = -1\rangle \leftrightarrow |F = 2, m_F = +1\rangle$). As a result, when the resonance is excited using both pairs of ground states simultaneously, the linear dependence on magnetic field of the center point of the resonance vanishes. The presence of a small magnetic field therefore produces only a broadening of the overall resonance. Kazakov et al. (2005a) have proposed using this mechanism to produce a pseudoresonance by applying a magnetic field large enough that the resonances on the individual pairs of ground states are shifted such that there is a dip in the center to which an LO can be stabilized.

The main perceived drawback of this technique is that it was predicted to be effective only in ^{87}Rb (or other atoms that have a nuclear spin of 3/2) atoms but not in ^{133}Cs (which has nuclear spin 7/2). Atoms with

larger nuclear spin have a greater number of levels in the excited state, which cause additional Lambda systems to be excited that destroy the CPT resonance through destructive interference. This is due to the fact that it requires selective excitation of the Lambda system by use of the $F' = 1$ excited state. This requires the use of very low buffer gas pressures, possibly in combination with a wall coating to reduce the wall-induced relaxation. Interestingly, high-contrast resonances have been observed using a similar scheme in a cell containing ^{133}Cs and a low buffer gas pressure (Watabe et al., 2009). This experimental result suggests that the excitation of multiple Lambda systems affects the resonance contrast only modestly.

3.2.4 The Use of End Resonances

The diluted atomic population participating in the clock transition can be improved by use of optical pumping, for example, with π-polarized light, as mentioned in Section 3.2.1 above. Ideally, the population accumulates in the $m_F = 0$ states, which are first-order magnetically insensitive. However, population can also be pumped into the "end" $m_F = F$ states, which can then be used to measure the hyperfine frequency. Because transitions between end states are first-order sensitive to magnetic fields, the local magnetic field must be measured simultaneously in a precise manner in order to reduce the field dependence of the clock output frequency. This can be done by measuring the Zeeman resonance frequency simultaneously with the hyperfine end-resonance frequency.

An additional advantage gained by the use of end resonances is the suppression of spin-exchange broadening. At high alkali atom densities, spin-exchange collisions can be the dominant source of hyperfine relaxation (Walter & Happer, 2002). An atomic sample perfectly polarized in the end state does not undergo spin-exchange relaxation because all atoms are oriented in the same direction, and therefore no angular momentum can be exchanged between any two colliding atoms. However, a small population in other states creates some relaxation, and hence only a partial suppression of the spin-exchange relaxation can be achieved in real atomic systems.

A final advantage of this scheme is that atoms can be optically pumped even at very high buffer gas pressures where the optical transitions from the ground-state hyperfine levels are broadened far beyond the state frequency splitting. The traditional OMDR configuration has considerably degraded performance in the presence of high buffer gas pressure, because the hyperfine optical pumping is very inefficient.

This proposal and accompanying experiments in ^{87}Rb are described by Jau et al. (2004b) and shown schematically in Figure 16. Microwave excitation of the hyperfine transitions was used in the experiment, as opposed to CPT transitions, although the enhanced contrast and narrow

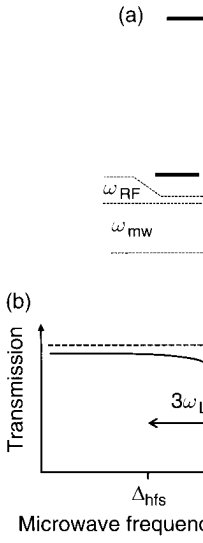

Figure 16 "End-resonance" meth
decreasing the line width of CPT r
"end" state with maximal angular
pumping light through the cell. A
simultaneously and the pump ligh
and (c) ω_{RF}, providing a simultane

line width should be equal
suppression by a factor of ab
enhanced signal contrast (Po
a magnetically sensitive hyp
cession frequency by use of
and Happer (2005). When th
short-term instability of 6×1
package (Braun et al., 2007).

3.2.5 Amplitude-Modulate Excitation Sources

CPT resonances are often exc
the order of 1 cm. In order
coherence due to wall collisi
The buffer gas species can b
relaxation rate is rather sm
roughly as the inverse of th
sion-induced relaxation wi

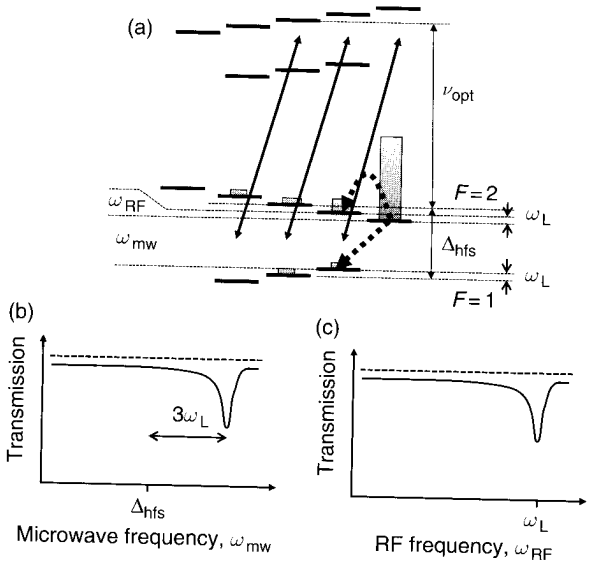

Figure 16 "End-resonance" method for increasing the absorption contrast and decreasing the line width of CPT resonances. (a) Atoms are optically pumped into the "end" state with maximal angular momentum, resulting in high transmission of the pumping light through the cell. A microwave field ω_{mw} and RF field ω_{RF} are applied simultaneously and the pump light transmission monitored as a function of (b) ω_{mw} and (c) ω_{RF}, providing a simultaneous measurement of ω_L and $\Delta_{hfs} - 3\,\omega_L$ (for ^{87}Rb)

line width should be equally present in CPT resonances. Line width suppression by a factor of about three was measured, as was considerably enhanced signal contrast (Post et al., 2003). Simultaneous measurement of a magnetically sensitive hyperfine transition frequency and Larmor precession frequency by use of a "tilted 0-0 state" was demonstrated by Jau and Happer (2005). When the system was operated as an atomic clock, a short-term instability of $6 \times 10^{-11}/\sqrt{\tau}$ was obtained in a compact physics package (Braun et al., 2007).

3.2.5 Amplitude-Modulated Versus Frequency-Modulated CPT Excitation Sources

CPT resonances are often excited in alkali vapor cells with dimensions on the order of 1 cm. In order to prevent rapid relaxation of the hyperfine coherence due to wall collisions, a buffer gas is usually added to the cell. The buffer gas species can be chosen so that its effect on the hyperfine relaxation rate is rather small. The optimal buffer gas pressure varies roughly as the inverse of the smallest cell dimension and balances collision-induced relaxation with relaxation caused by residual diffusion

through the buffer gas to the walls of the cell (Kitching et al., 2002; Knappe, 2007).

The buffer gas also significantly broadens the optical transitions involved in the CPT resonance. As the buffer gas pressure is increased, the optical transitions from the ground-state hyperfine levels can go from being completely resolved to being completely unresolved. When a single modulated laser is used to excite the resonances, the number of modulation sidebands that interact with the atoms can vary from two to many. In Figure 17a, the spectrum from the optical transitions is plotted in these

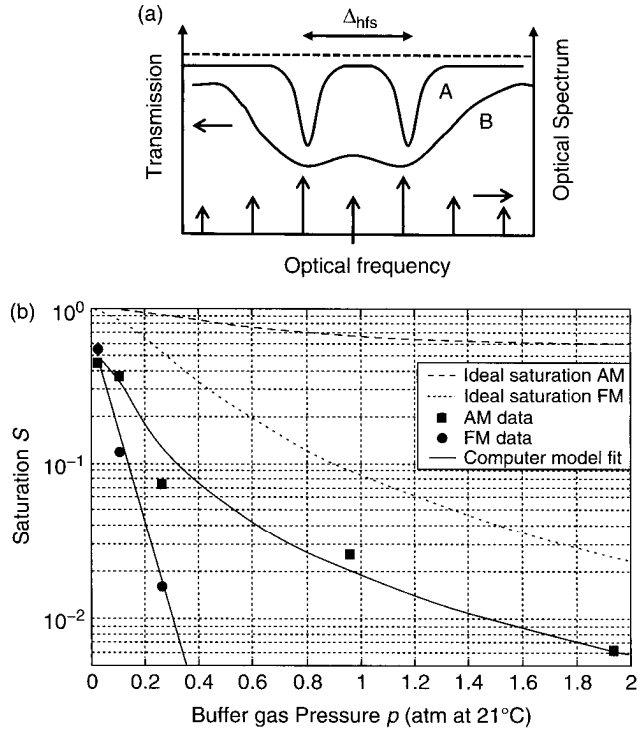

Figure 17 (a) Comparison of atomic optical absorption spectrum with laser modulation spectrum for two qualitatively different buffer gas pressures. Trace A is for a low buffer gas pressure, for which the optical transitions from each hyperfine level are well resolved, while Trace B is for a higher buffer gas pressure, for which the transitions are not resolved. For the case of Trace A, only two of the frequencies in the optical spectrum interact with the atoms, while for the case of Trace B, almost all do. (b) Experimental data comparing the strength of the CPT resonance (identified with the saturation parameter *S*) as a function of buffer gas pressure for FM- and AM-modulated light fields. Reprinted figure with permission from Post et al. (2005); © 2005 of the American Physical Society

two limits and compared with t
one-half the hyperfine splitting

When the transitions are reso
interact with the atoms (Trace A
a phase defined by the relative p
the absorption contrast can be q
are not resolved, many optical fr
in Figure 17), and the dark state
the phase of each pair of sideban
the light source is amplitude mo
sidebands has the same phase
independently add constructive
contrast. If, on the other hand,
some pairs of sidebands are out
states add destructively. For th
small vapor cells, therefore, the
are critically important. A carefu
by Post et al. (2005), largely sup
here. Data from Post et al. (2005

3.3 High-Contrast Resonances

One of the issues associated with
transmission contrast of the CPT
of a few percent) when the atom
several reasons, including the
wave laser modulation that do
resonances. A very large fractio
clock performance can be elimin
Shah et al. (2007) demonstrated
mixing in a double-Lambda sy
most of the background light fa

The experimental setup from
In this experiment, the $\sigma+$ light
in atoms by use of conventional
single-frequency laser with opp
generated in the atoms is gently
jugate light field whose frequen
probe beam by the ground-sta
spectral and polarization filterin
fields other than the conjugate
the pump beams satisfy the tw
brightness observed on the pho
field. When the two-photon con

alls of the cell (Kitching et al., 2002;

ntly broadens the optical transitions
s the buffer gas pressure is increased,
ound-state hyperfine levels can go from
completely unresolved. When a single
he resonances, the number of modula-
ne atoms can vary from two to many. In
e optical transitions is plotted in these

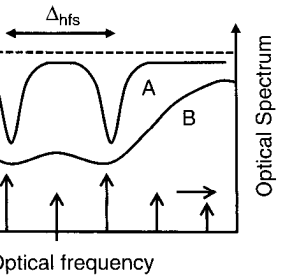

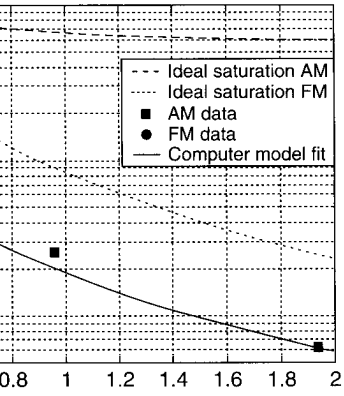

tical absorption spectrum with laser
ly different buffer gas pressures. Trace A is for
optical transitions from each hyperfine level
higher buffer gas pressure, for which the
e of Trace A, only two of the frequencies in the
s, while for the case of Trace B, almost all do.
ength of the CPT resonance (identified with the
buffer gas pressure for FM- and AM-
with permission from Post et al. (2005); © 2005

two limits and compared with the spectrum of a light field modulated at one-half the hyperfine splitting.

When the transitions are resolved and only two optical field frequencies interact with the atoms (Trace A in Figure 17a), a dark state is created with a phase defined by the relative phase of the two relevant optical fields, and the absorption contrast can be quite large. However, when the transitions are not resolved, many optical frequencies interact with the atoms (Trace B in Figure 17), and the dark state tries to adjust its phase to correspond to the phase of each pair of sidebands separated by the hyperfine splitting. If the light source is amplitude modulated, the beatnote between each pair of sidebands has the same phase and the dark states created by each pair independently add constructively to form a single dark state with high contrast. If, on the other hand, the light source is frequency modulated, some pairs of sidebands are out of phase with the other pairs, and the dark states add destructively. For the high buffer gas pressures required for small vapor cells, therefore, the modulation properties of the light source are critically important. A careful study of this phenomenon is presented by Post et al. (2005), largely supporting the intuitive reasoning presented here. Data from Post et al. (2005) are shown in Figure 17b.

3.3 High-Contrast Resonances Using Four-Wave Mixing

One of the issues associated with microwave CPT atomic clocks is that the transmission contrast of the CPT resonance is typically small (in the range of a few percent) when the atomic clock is fully optimized. This is due to several reasons, including the presence of modes generated by microwave laser modulation that do not participate in the formation of CPT resonances. A very large fraction of the laser noise that affects the CPT clock performance can be eliminated by removing the background light. Shah et al. (2007) demonstrated a novel technique based on four-wave mixing in a double-Lambda system, shown in Figure 18a, to eliminate most of the background light falling on the photodetector.

The experimental setup from Shah et al. (2007) is shown in Figure 18b. In this experiment, the $\sigma+$ light is used to create a dark state (coherence) in atoms by use of conventional CPT laser modulation. By use of a second single-frequency laser with opposite circular polarization, the coherence generated in the atoms is gently probed to stimulate emission of a conjugate light field whose frequency is separated from that of the original probe beam by the ground-state splitting. Through a combination of spectral and polarization filtering, the power in all of the incident light fields other than the conjugate field is then largely eliminated. When the pump beams satisfy the two-photon resonance condition, there is brightness observed on the photodetector from the incident conjugate field. When the two-photon condition is not satisfied, the conjugate field

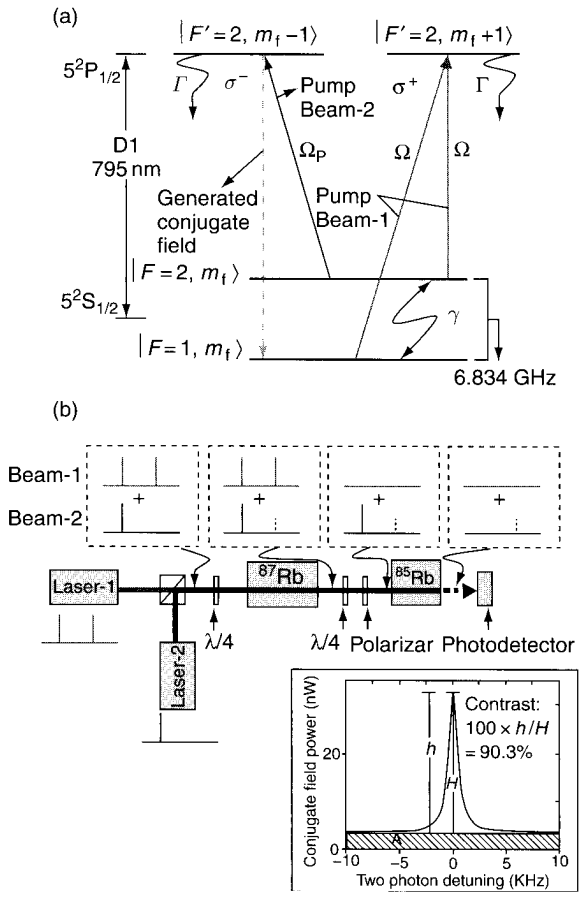

Figure 18 (a) Level diagram showing the polarizations and tunings of the optical fields for CPT resonance contrast enhancement using four-wave mixing and a filter cell. (b) Experimental setup and contrast measurement. From Shah et al. (2007); reproduced with permission from the Optical Society of America

is not generated, and therefore there is no light incident on the photodetector. Experimentally the transmission contrast seen in this way approaches 95% and is limited only by the efficiency of the optical filtering in the setup.

3.4 Push–Pull Laser Atomic Oscillator

Jau and Happer (2007) have demonstrated a novel technique in which they show a "mode-locking" type behavior in a laser cavity in the presence of alkali atoms. In this self-oscillating system, the frequency

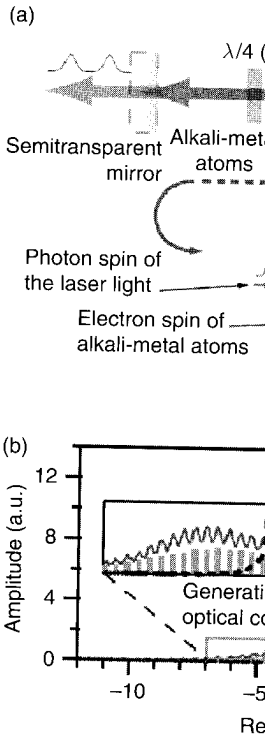

Figure 19 (a) Operation of the "push–p
output frequencies spaced by the hyper
Reprinted figure with permission from J
Physical Society

separation of the spontaneously g
state $m_F = 0 \rightarrow m_F = 0$ transition fr
operating the system as an atomi
mental setup is shown in Figure 1

The basic idea is the following:
prepared in a dark state between t
atoms in the dark state precess a
continuously transparent only to li
Two or more optical modes that ar
and have a constant phase relatio
Lambda system are thus the "al
Because of the fixed phase relatio
cavity operation is analogous to th
that the light coupled out of the ca
to that of a frequency comb (see Fi

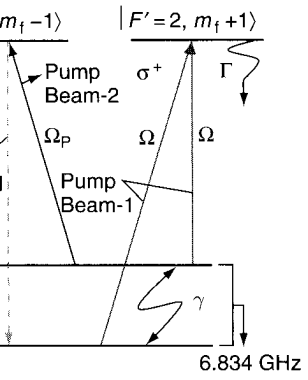

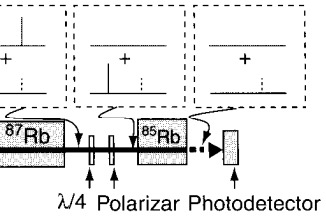

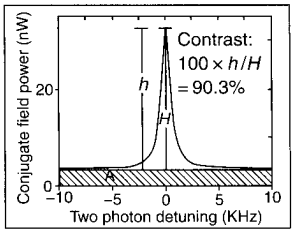

he polarizations and tunings of the optical fields
ent using four-wave mixing and a filter cell.
asurement. From Shah et al. (2007); reproduced
ety of America

here is no light incident on the photo-
ansmission contrast seen in this way
nly by the efficiency of the optical filter-

cillator

monstrated a novel technique in which
be behavior in a laser cavity in the pre-
self-oscillating system, the frequency

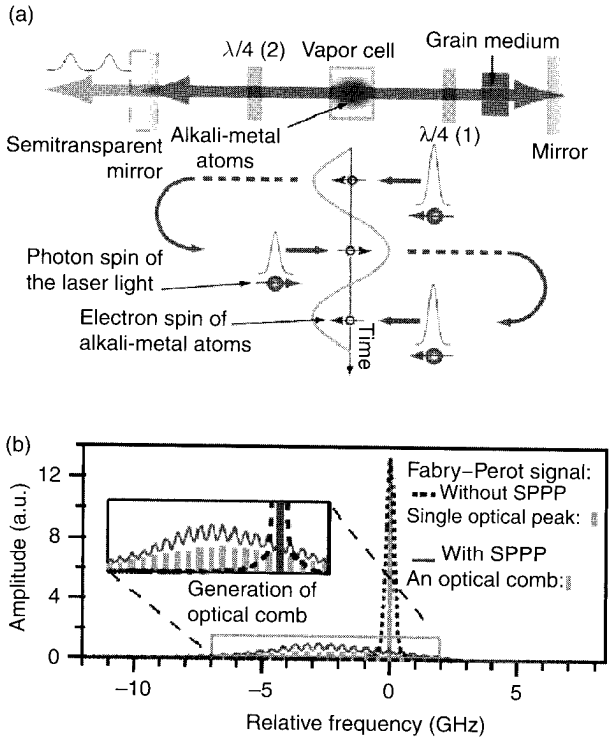

Figure 19 (a) Operation of the "push–pull" laser-atomic oscillator. (b) The comb of output frequencies spaced by the hyperfine frequency of the alkali atoms in the cavity. Reprinted figure with permission from Jau and Happer (2007); © 2007 of the American Physical Society

separation of the spontaneously generated modes is given by the ground state $m_F = 0 \rightarrow m_F = 0$ transition frequency, introducing the prospects of operating the system as an atomic clock. The schematic of their experimental setup is shown in Figure 19a.

The basic idea is the following: imagine that all the atoms are initially prepared in a dark state between the $m_F = 0$ hyperfine ground states. The atoms in the dark state precess at the hyperfine frequency and appear continuously transparent only to light fields that excite a Lambda system. Two or more optical modes that are separated by the hyperfine frequency and have a constant phase relation between them suitable for exciting a Lambda system are thus the "allowed" cavity modes in the system. Because of the fixed phase relationship between the optical modes, the cavity operation is analogous to that in a mode-locked laser. The result is that the light coupled out of the cavity has a frequency spectrum similar to that of a frequency comb (see Figure 19b).

Through the use of two $\lambda/4$ wave plates, the optical arrangement in the cavity was such that the light excites $\sigma+$ transitions traveling along one direction and $\sigma-$ transitions when traveling in the opposite direction. The purpose of this was to prepare atoms in a pure superposition of $m_F = 0$ states without the usual fraction in the end state. The length of the cavity was chosen to be an odd integral multiple of half the hyperfine wavelength, such that the dark state due to oppositely traveling light fields remained in phase. This system has the important feature that no LO is needed to excite the resonance; the system here is an active system and oscillates at the hyperfine frequency.

A related experiment was described by Akulshin and Ohtsu (1994), in which an alkali cell was placed in an external cavity providing optical feedback to a distributed feedback (DBF) laser. A second laser beam, separated in frequency by approximately the alkali ground-state hyperfine frequency, was sent through the cell parallel to the first laser beam. It was found that the laser with feedback optically locked to the second laser with a frequency difference exactly equal to the ground-state hyperfine splitting. CPT-induced polarization rotation has also been used in a similar context (Liu et al., 1996).

A number of other self-oscillating systems based on CPT have been developed (Strekalov et al., 2003, 2004; Vukicevic et al., 2000), in which RF rather than optical feedback was used to sustain the oscillation.

3.5 The CPT Maser

A CPT maser (Godone et al., 1999; Vukicevic et al., 2000) is an active frequency standard in which a coherent microwave signal is directly recovered from the atoms instead of an indirect signal in the form of change in optical transmission. This approach can also eliminate the need for an external microwave oscillator for laser modulation. Once the microwave oscillation is started, it can be sustained indefinitely by use of the microwaves obtained directly from the atoms in a feedback configuration.

In a CPT maser, atoms are enclosed in a microwave cavity whose frequency is tuned close to the difference frequency between the $m_F = 0$ hyperfine ground states (see Figure 20). The coherence generated in the atoms through dark-state excitation couples with one of the cavity modes to stimulate emission of microwaves by the atoms at the hyperfine frequency. The microwaves emitted by the atoms can, in turn, be used to modulate the laser to sustain the maser operation.

A complete CPT maser prototype was demonstrated and evaluated and an instability of $3\times10^{-12}/\sqrt{\tau}$ was measured, integrating down to below 10^{-13} at 1 hour, once the linear drift had been removed (Levi et al., 2004). A variety of noise contributions were also measured, with thermal

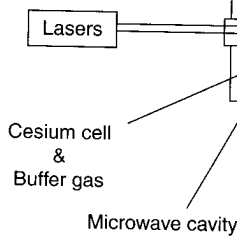

Figure 20 The CPT maser, in which a
using CPT and the power radiated by th
in a microwave cavity. Experimental se
Vanier et al. (1998); © 1998 of the Ame

noise being the most imp
and temperature-related effects
Considerable theoretical work w
operation of the CPT maser in d
1998), as well as a number of inte
to its operation and underlying p

3.6 N-Resonance

A novel alternative to CPT, the N-
2005) and studied subsequently (
which has its origins in earlier wo
atoms (Zibrov et al., 2002), can
conventional OMDR technique.
are optically pumped into one h
field resonant with a transition fr

However, instead of exciting
microwave field, a bichromatic
resonance with the microwave tr
transition. When the Raman reso
optically pumped back into the
increased optical absorption of the
is in contrast with the conventio
absorption is seen when the two-

Among the advantages of the N
resonance, this scheme produces s
transmission contrast) on both th
stabilities of $1.5 \times 10^{-10}/\sqrt{\tau}$ have

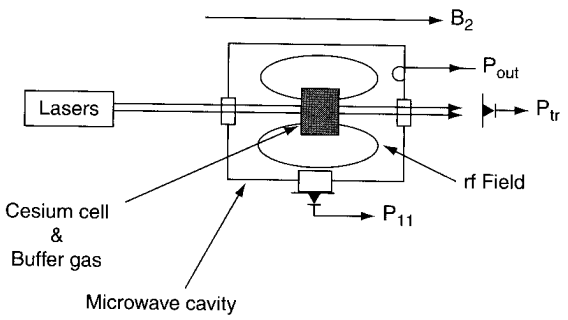

Figure 20 The CPT maser, in which a ground-state atomic coherence is generated using CPT and the power radiated by the corresponding magnetic moment, is captured in a microwave cavity. Experimental setup. Reprinted figure with permission from Vanier et al. (1998); © 1998 of the American Physical Society

noise being the most important at short integration times and temperature-related effects dominating at long integration times. Considerable theoretical work was also carried out to understand the operation of the CPT maser in detail (Godone et al., 2000; Vanier et al., 1998), as well as a number of interesting independent phenomena related to its operation and underlying physics (Godone et al., 2002a,b,c,d).

3.6 N-Resonance

A novel alternative to CPT, the N-resonance, was proposed (Zibrov et al., 2005) and studied subsequently (Novikova et al., 2006a,b). This scheme, which has its origins in earlier work on multiphoton resonances in alkali atoms (Zibrov et al., 2002), can be thought of as a modification of the conventional OMDR technique. Just as in the OMDR technique, atoms are optically pumped into one hyperfine level with an optical "probe" field resonant with a transition from the other hyperfine level.

However, instead of exciting the microwave transition by use of a microwave field, a bichromatic optical field is used, close to Raman resonance with the microwave transition, but detuned from the optical transition. When the Raman resonance condition is achieved, atoms are optically pumped back into the depleted hyperfine level, leading to increased optical absorption of the pump field. This absorptive resonance is in contrast with the conventional CPT resonance, in which reduced absorption is seen when the two-photon condition is satisfied.

Among the advantages of the N-resonance scheme is that unlike CPT resonance, this scheme produces signals of high contrast (as high as 30% transmission contrast) on both the D1 and the D2 transitions. Clock in stabilities of $1.5 \times 10^{-10}/\sqrt{\tau}$ have been obtained in ^{87}Rb confined in a cell

of diameter 2.5 cm. It has also been shown that despite the inherently off-resonant operation of N-resonance-based atomic clocks, the light shifts can be canceled to first order by appropriately choosing the intensity in the pump and the probe beams, allowing the possibility of building an atomic clock with good long-term stability based on N-resonances. This scheme still requires that the excited-state hyperfine resonances be resolved, and hence has the same limitations with respect to buffer gas pressure as some of the techniques discussed above.

Although in its most general form requiring optical fields at three unique frequencies, this scheme can be implemented by use of only two optical fields by allowing a single field to do double duty, both as the probe field and as one of the legs of the Raman field. An energy-level diagram of the N-resonance excitation mechanism is shown in Figure 21a, and the experimental implementation using a single modulated diode laser is shown in Figure 21b. One of the weak sidebands generated by the modulator serves as the probe and one of the Raman fields, while the strong optical carrier provides the second Raman field. An etalon is placed after the cell to attenuate the strong Raman field and therefore increase the resonance contrast.

3.7 Raman–Ramsey Pulsed CPT

As described above, light shifts play a major role in determining the long-term stability of vapor cell atomic clocks. In CPT clocks, the presence of the off-resonant optical modes and an imbalance between the intensities in the two arms of the Lambda system can cause significant light shifts. A commonly used technique to avoid light shifts is to pulse the light fields and allow the atoms to evolve in the dark. An additional advantage of pulsing the light fields is that atoms can be prepared in a coherent superposition state with higher efficiency by use of strong light fields while avoiding power broadening to a large extent. A pulsed technique for CPT clocks has also been recently proposed (Zanon et al., 2004b, 2005) and demonstrated (Guerandel et al., 2007), and it has shown excellent both stability (Boudot et al., 2009) and a high degree of insensitivity to light shifts (Castagna et al., 2009).

In this technique, the light fields are switched on and off at regular intervals. The operation of the clock can be understood as follows: during the first pulse, CPT light fields prepare atoms in a coherent dark state. After the state preparation is nearly complete, the light fields are turned off for a period roughly equal to the ground-state relaxation time. During this period, the atoms freely evolve at the ground-state hyperfine frequency without being perturbed by the light fields.

When the second light pulse is turned on, the hyperfine frequency of the atoms in the dark is inferred from the initial absorption signal of the light by the atoms. If the frequency of the microwave oscillator used to modulate the light fields is the same as that of the atomic hyperfine frequency (in the

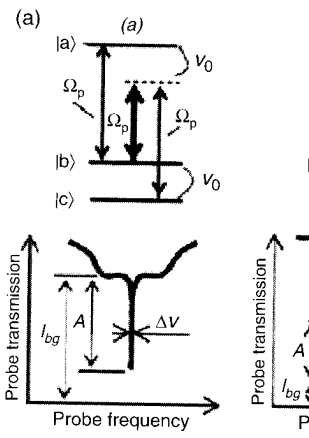

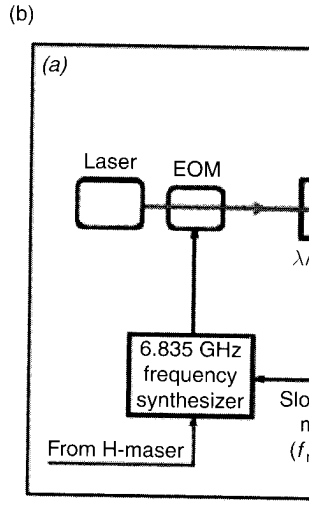

Figure 21 (a) Atomic level diagram fo
implementation. Reprinted figure with
the American Physical Society

dark), then the atoms appear trans
are turned on. This is because the
the atomic evolution in the dark
continue to appear transparent to t
pulse repumps the fraction of th
when the light fields were turned
atomic energy level diagram are
experimentally observed Ramsey

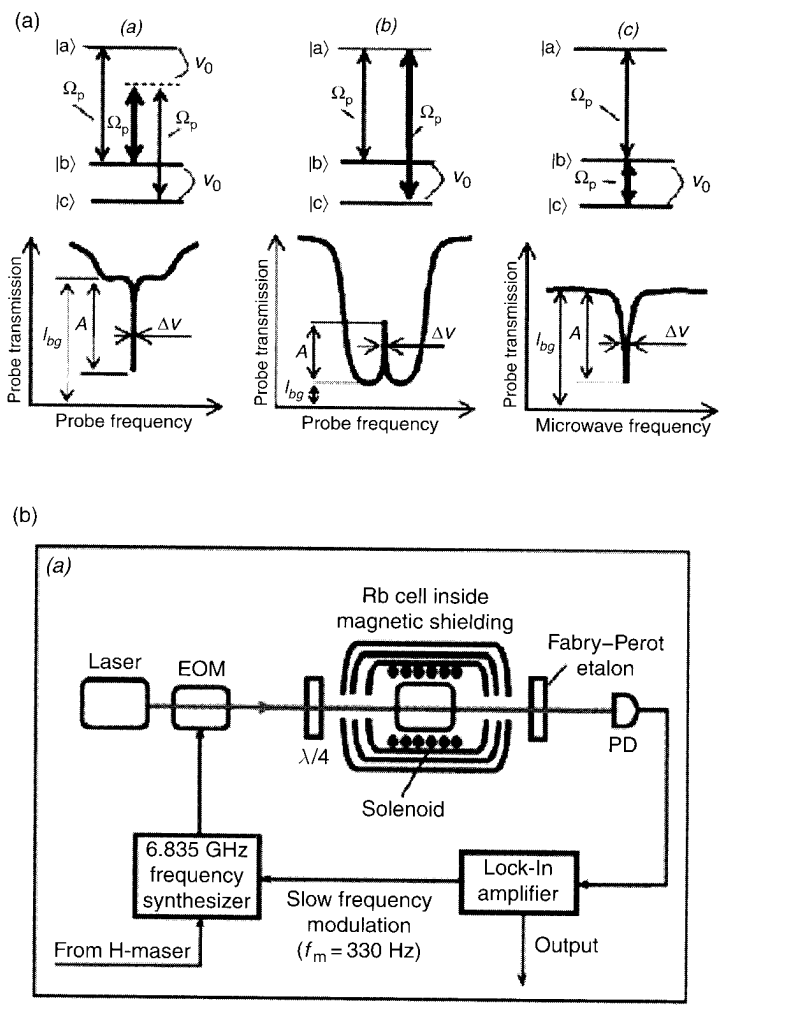

Figure 21 (a) Atomic level diagram for the N-resonance. (b) Experimental implementation. Reprinted figure with permission from Zibrov et al. (2005); © 2005 of the American Physical Society

dark), then the atoms appear transparent to the light fields the instant they are turned on. This is because the microwave modulation on the laser and the atomic evolution in the dark remain in phase; as a result, the atoms continue to appear transparent to the light fields. The later part of the second pulse repumps the fraction of the atoms that relaxed during the period when the light fields were turned off. The pulsed excitation scheme and atomic energy level diagram are shown in Figure 22a. Figure 22b shows experimentally observed Ramsey fringes when the CPT clock is operated in

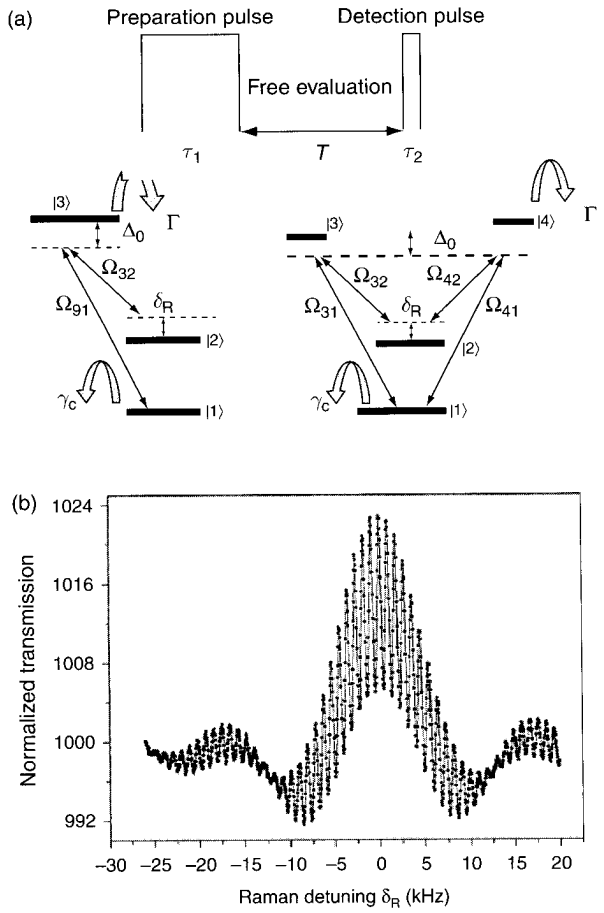

Figure 22 Raman–Ramsey excitation of hyperfine clock transitions. (a) Pulsed excitation scheme and atomic energy spectrum. (b) Raman–Ramsey pulses. Reprinted figure with permission from Zanon et al. (2005); © 2005 of the American Physical Society

the pulsed mode. The individual fringe width can be narrower than the width of a zero-intensity continuously-excited CPT resonance if the delay between successive pulses is greater than the ground-state relaxation time.

The pulsed CPT interrogation scheme has been operated as an atomic frequency reference and studied in some detail. It was shown that both the short-term frequency stability and the light shift could be improved considerably compared to continuous interrogation in the pulsed configuration (Castagna et al., 2007). A short-term instability of $7\times10^{-13}/\sqrt{\tau}$ was obtained, integrating down to 2×10^{-14} at 1000 seconds when the linear frequency drift was removed. Dominant contributions to the

short-term instability were amp
noise in the photodetection syst

Recently, "pulsed" vapor ce
clocks in which the optical pu
applied at different times, have
(Godone et al., 2004, 2006a,b). In
tion of pulsed CPT excitation of
the buffer gas shifts present in va
et al., 2003, 2004a). A novel sy
hyperfine coherence and feedfo
also been investigated (Guo et a

3.8 CPT in Optical Clocks

So far we have focused on the
clocks. In recent years, CPT-base
or the terahertz regime have be
et al., 2005; Yoon, 2007). Optica
microwave clocks that the transit
of the resonances, are orders o
narrow line widths, forbidden t
lines in alkaline earth atoms are
such as the $^1S_0 \leftrightarrow {}^3P_0$ line at 698 n
order and cannot be accessed b
however, possible to observe th
photon (CPT) excitation as show

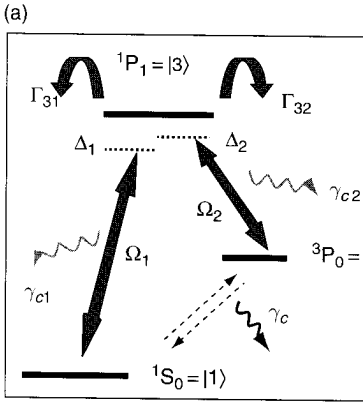

Figure 23 CPT excitation of intercomb
(a) Atomic level structure and optical fi
figure with permission from Zanon-Wil
Physical Society

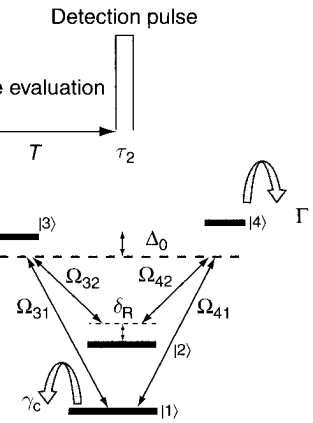

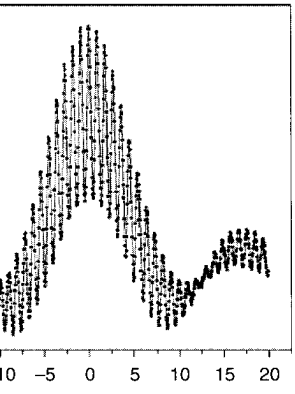

hyperfine clock transitions. (a) Pulsed
ctrum. (b) Raman–Ramsey pulses. Reprinted
2005); © 2005 of the American Physical Society

ringe width can be narrower than the
ısly-excited CPT resonance if the delay
r than the ground-state relaxation time.
cheme has been operated as an atomic
n some detail. It was shown that both
and the light shift could be improved
ous interrogation in the pulsed config-
short-term instability of $7\times10^{-13}/\sqrt{\tau}$
to 2×10^{-14} at 1000 seconds when
noved. Dominant contributions to the

short-term instability were amplitude noise on the laser and electronic noise in the photodetection system.

Recently, "pulsed" vapor cell atomic clocks, conventional OMDR clocks in which the optical pumping field and microwave field are applied at different times, have also been the subject of some research (Godone et al., 2004, 2006a,b). In addition, there has been some consideration of pulsed CPT excitation of cold atom systems in order to eliminate the buffer gas shifts present in vapor cell clocks (Farkas et al., 2009; Zanon et al., 2003, 2004a). A novel system based on transient excitation of a hyperfine coherence and feedforward to correct the LO frequency has also been investigated (Guo et al., 2009).

3.8 CPT in Optical Clocks

So far we have focused on the role of CPT resonances in microwave clocks. In recent years, CPT-based atomic clocks operating in the optical or the terahertz regime have been proposed (Hong et al., 2005; Santra et al., 2005; Yoon, 2007). Optical clocks have the great advantage over microwave clocks that the transition frequencies, and hence the Q-factors of the resonances, are orders of magnitude higher. In order to obtain narrow line widths, forbidden transitions such as the intercombination lines in alkaline earth atoms are often used. Some of these transitions, such as the $^1S_0 \leftrightarrow {}^3P_0$ line at 698 nm in bosonic ^{188}Sr, are forbidden to any order and cannot be accessed by use of single-photon excitation. It is, however, possible to observe the transition indirectly by use of two-photon (CPT) excitation as shown in Figure 23. The line width of the

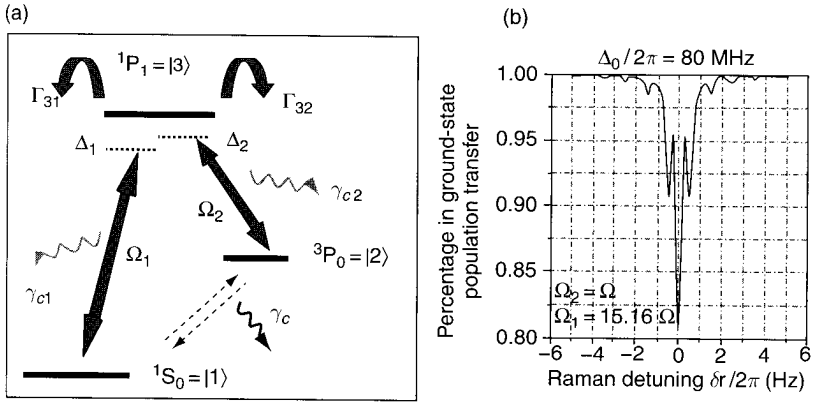

Figure 23 CPT excitation of intercombination transitions in alkaline earth atoms. (a) Atomic level structure and optical fields. (b) Predicted Raman lineshape. Reprinted figure with permission from Zanon-Willette et al. (2006); © 2006 of the American Physical Society

transition can be conveniently tuned from megahertz to below 1 Hz by controlling the power broadening of this transition. It has been predicted that the accuracy of such a clock can be better than 10^{-17}. To eliminate light shifts, a pulsed CPT scheme similar to the scheme proposed for microwave clocks (see pulsed CPT section above) has been proposed and demonstrated (Zanon-Willette et al., 2006).

4. ADDITIONAL CONSIDERATIONS

4.1 Light-Shift Suppression

Several interesting techniques have been developed to reduce the effects of light shift on the long-term instability of vapor cell atomic clocks. One such scheme involves the use of the multiplicity of sidebands created when the injection current of a diode laser is modulated (Zhu & Cutler, 2000). Current modulation of a diode laser results in both AM and FM modulation of the output optical field. As the modulation index is increased, a comb of optical frequencies is therefore produced, separated from the carrier by multiples of the modulation frequency. Each of these optical frequencies produces a light shift for each of the ground-state hyperfine frequencies, and each shift can be either positive or negative, depending on the detuning of the specific frequency from the relevant transition. By adjusting the modulation index, it is therefore possible to modify the light shift and reduce it to near zero. A calculation from Zhu and Cutler (2000) is shown in Figure 24a, indicating that for two different operating conditions, the first-order light shift is reduced to zero at a modulation index of about 2.5. Measurements shown in Figure 24b confirm the effect. A frequency instability of about 10^{-13} was obtained at an integration period of 1000 seconds by use of this technique (Zhu & Cutler, 2000). It should be noted that, in principle, this same technique can be used to reduce or eliminate the light shift in OMDR clocks (Affolderbach et al., 2003). However, the required modulation of the laser injection current would have to be added to this configuration, while this is present quite naturally in the CPT configuration.

The technique above allows for the modulation index to be set such that small changes in the light intensity do not (to first order) affect the clock frequency. Such changes in light intensity can occur, for example, if the laser generating the optical fields ages in some way. However, this aging can also result in a change in the electrical impedance of the laser. If the laser impedance changes, the coupling of the RF modulation field to modulation on the optical field in general changes. As shown in Figure 24b, a change in the coupled RF power by 1 dB can result in a frequency shift on the order of 10^{-10}.

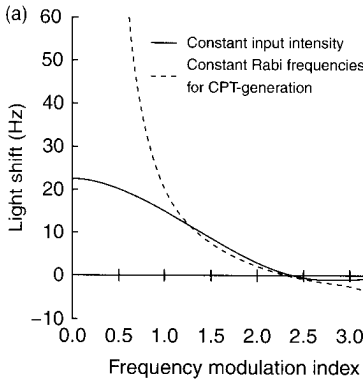

Figure 24 Suppression of light shif
(a) Theoretical predictions of the ligl
(b) Measurements of the frequency
several values of the modulation ind
$I \sim 40\,\mu$}go:goW/cm^2. Operation of th
long-term frequency stability when
permission from Zhu and Cutler (20

In order to address the effe
modification of the RF modula
2006a). After adjusting the RF
power of the light field is mo
experiment) by use of a variab
will cause a corresponding char
the zero-light-shift condition is
frequency is more stable than
quency, the modulated frequen
comparison of synthesizer freq
power can then be corrected to
schematic of the optical/electr
Under exaggerated conditions,
output frequency to RF imped
temperature) by a factor of 10 i

4.2 Laser Noise Cancellation

One of the problems frequently
rogation is the conversion of la
detector output by the optica
which otherwise cannot be see
the atoms act as a sharp disc
vicinity of the optical resonan

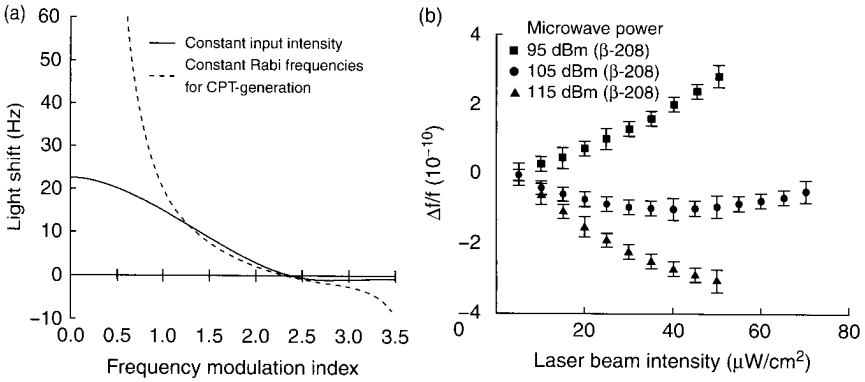

Figure 24 Suppression of light shifts using optimized modulation of a diode laser. (a) Theoretical predictions of the light shift as a function of madulation index. (b) Measurements of the frequency shift as a function of laser beam intensity for several values of the modulation index. A local minimum is observed for $\beta \sim 2.33$ and $I \sim 40\mu$}go:goW/cm^2. Operation of the clock at this setpoint should result in improved long-term frequency stability when light shifts dominate. Reprinted figure with permission from Zhu and Cutler (2000)

In order to address the effects of such changes in laser impedance, a modification of the RF modulation technique was suggested (Shah et al., 2006a). After adjusting the RF power to the zero-light-shift point, the power of the light field is modulated at a low frequency (17 Hz in this experiment) by use of a variable attenuator. This modulation in intensity will cause a corresponding change in the frequency of the CPT resonance if the zero-light-shift condition is not satisfied. Assuming that the synthesizer frequency is more stable than the CPT resonance at the modulation frequency, the modulated frequency shift can be detected through the normal comparison of synthesizer frequency to CPT resonance frequency. The RF power can then be corrected to maintain the zero-light-shift condition. A schematic of the optical/electronic arrangement is shown in Figure 25. Under exaggerated conditions, an improvement in the insensitivity of the output frequency to RF impedance (as adjusted by modulating the laser temperature) by a factor of 10 is obtained (Shah et al., 2006a).

4.2 Laser Noise Cancellation

One of the problems frequently encountered in laser-based atomic interrogation is the conversion of laser frequency noise to current noise in the detector output by the optical resonance. The laser frequency noise, which otherwise cannot be seen by the photodetector, appears because the atoms act as a sharp discriminator of the optical frequency in the vicinity of the optical resonance. The amount of noise that appears on

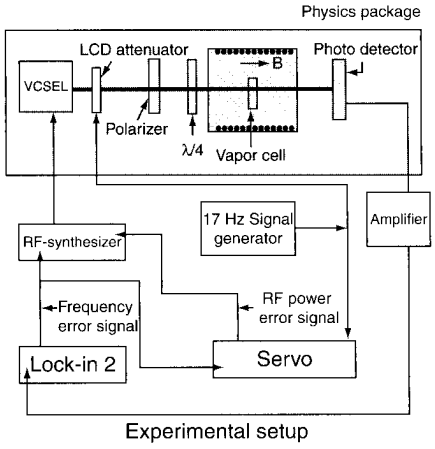

Figure 25 Schematic of a technique to maintain the RF power at the zero-light-shift point as the laser impedance ages. Reprinted figure with permission from Shah et al. (2006a); © 2006 of the Optical Society of America

the photodetector signal depends on the amount of frequency noise present on the light (the laser line width), the width of the optical resonance, and the tuning of the laser frequency.

There are several solutions with varying complexity that can be used to reduce this excess laser frequency to photodetector current noise. Among the simplest is to choose a laser with a narrow line width. However, this is not always feasible for commercial or other technical reasons. Another simple alternative is to broaden the optical resonance using higher buffer gas pressure which reduces the slope of frequency discrimination by the optical resonance. Here again, there are limitations since buffer gas pressure cannot be arbitrarily increased without affecting the clock performance. For example, in the regime in which most CPT/OMDR clocks operate, one of the immediate consequences of using higher buffer gas pressure is that the optical depth of the atomic medium at a given temperature is correspondingly reduced. To compensate for the loss in the optical depth, the atomic vapor pressure can be increased by increasing the cell temperature. But this increases the width of the ground-state resonance by increasing alkali–alkali spin-exchange contribution to the ground-state relaxation.

Another alternative to reducing the laser noise is to use external means such as real-time laser noise cancellation using differential detection. This was accomplished, for example, by Gerginov et al. (2008). Here, a split wave plate was used such that light in one half of the vapor cell was circularly polarized and light in the other half was linearly polarized (see Figure 26). The circular and the linear components of the light beam were collected on two spatially separated photodetectors. While the CPT

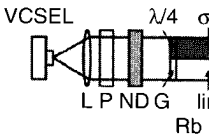

Figure 26 Experimental setup used
polarizer; ND, neutral density filter;
photodiode. Reprinted figure with p
IEEE

resonance is excited in only th
only by PD1, the laser noise ap
signals from the two photodete
affecting the CPT resonance see
been developed for OMDR clo
bluh et al., 2006).

Yet another technique for la
demonstrated by Rosenbluh
originating with the laser was
to the dark end state were sim
was excited using a combinat
larly polarized light obtained fr
equal to one quarter of the
between the right and the lef
After propagating the light thr
were separated using an arrang
polarizing beam splitter; each
tored using photodetectors. Du
polarization components of the
the phase of the coherent dar
combined is partially shifted
polarization components of th
but opposite signs for the two
try into the CPT resonance line
to an otherwise Lorenztian p
adding the signals from both p
lineshape (Figure 27a), the
(Figure 27b). Because differen
case, the common mode laser
the overall strength of the CPT
the oscilloscope traces of the C
has lower noise compared to Fi
not employed.

g

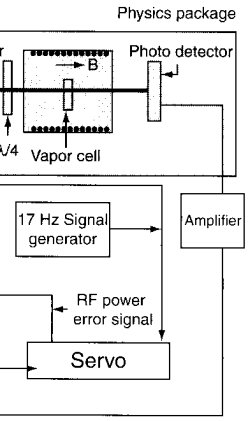

mental setup

maintain the RF power at the zero-light-shift
rinted figure with permission from Shah et al.
f America

ds on the amount of frequency noise
line width), the width of the optical
laser frequency.
a varying complexity that can be used to
to photodetector current noise. Among
th a narrow line width. However, this is
ial or other technical reasons. Another
ne optical resonance using higher buffer
lope of frequency discrimination by the
e are limitations since buffer gas pressure
nout affecting the clock performance. For
nost CPT/OMDR clocks operate, one of
ing higher buffer gas pressure is that the
m at a given temperature is correspond-
the loss in the optical depth, the atomic
increasing the cell temperature. But this
nd-state resonance by increasing alka-
n to the ground-state relaxation.
the laser noise is to use external means
llation using differential detection. This
by Gerginov et al. (2008). Here, a split
ight in one half of the vapor cell was
ne other half was linearly polarized (see
near components of the light beam were
rated photodetectors. While the CPT

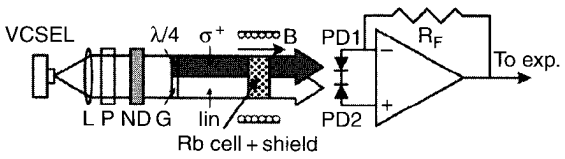

Figure 26 Experimental setup used to reduce the laser noise. VCSEL: L, lens; P, polarizer; ND, neutral density filter; $\lambda/4$, quarter-wave plate; G, glass plate $\sigma+$; PD, photodiode. Reprinted figure with permission from Gerginov et al. (2008); © 2008 of IEEE

resonance is excited in only the first part of the vapor cell and thus seen only by PD1, the laser noise appears in both the channels. Subtracting the signals from the two photodetectors thus removes the laser noise without affecting the CPT resonance seen using PD1. Similar techniques have also been developed for OMDR clocks (Deng, 2001; Mileti et al., 1998; Rosenbluh et al., 2006).

Yet another technique for laser noise cancellation was proposed and demonstrated by Rosenbluh et al. (2006). In this technique, the noise originating with the laser was reduced and the effects of optical pumping to the dark end state were simultaneously eliminated. A CPT resonance was excited using a combination of copropagating left and right circularly polarized light obtained from a common laser. A relative path delay, equal to one quarter of the microwave wavelength, was introduced between the right and the left circular components of the light beam. After propagating the light through the vapor cell, the two components were separated using an arrangement of a quarter-wave plate ($\lambda/4$) and a polarizing beam splitter; each of the components was separately monitored using photodetectors. Due to the $\lambda/4$ path delay between the two polarization components of the light beam that excite the CPT resonance, the phase of the coherent dark state that is excited by the two beams combined is partially shifted in phase with respect to the individual polarization components of the beam. This phase shift, which has equal but opposite signs for the two light components, introduces an asymmetry into the CPT resonance lineshape by adding a dispersive component to an otherwise Lorenztian profile. While the CPT resonance seen by adding the signals from both photodetectors still has a purely Lorenztian lineshape (Figure 27a), the difference signal is purely dispersive (Figure 27b). Because differential detection is employed in the latter case, the common mode laser noise is removed, without any effect on the overall strength of the CPT resonance signal. It can be seen even from the oscilloscope traces of the CPT resonances that the trace in Figure 27b has lower noise compared to Figure 27a, in which differential detection is not employed.

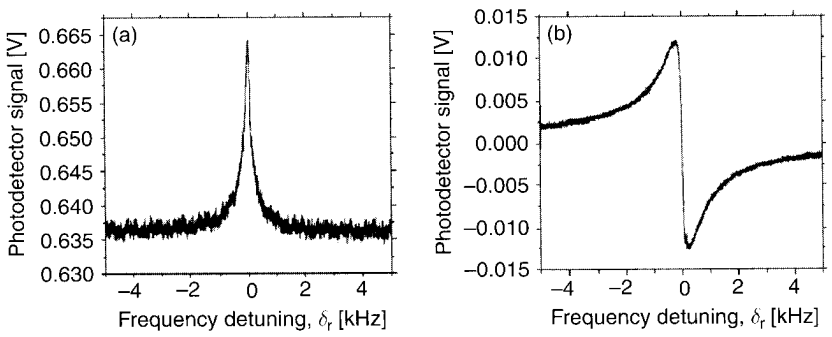

Figure 27 Lineshapes of atomic-coherence-induced resonances for phase-shifted, two-beam excitation. (a) One beam blocked, conventional CPT resonance, (b) both beams present, signals from balanced photodetectors subtracted. Reprinted figure with permission from Rosenbluh et al. (2006); © 2006 of the Optical Society of America

4.3 Light Sources for Coherent Population Trapping

A number of types of light sources have been used to generate the bichromatic optical field needed to excite hyperfine CPT resonances. Although the coherence requirements of the light source are not nearly as stringent as in optical spectroscopy, the lamps currently used in conventional atomic clocks appear to be too incoherent to generate CPT resonances of any reasonable contrast. The requirement on the coherence is nominally that the line width of the light source be smaller than the buffer gas broadened optical transitions in the alkali atoms, typically ranging from a few hundred megahertz to several tens of gigahertz. Most lasers satisfy this requirement, which allows great latitude in laser choice to optimize the system with respect to other criteria.

The earliest experiments on CPT were carried out using multimode dye lasers (Alzetta et al., 1976). Since then, a variety of more sophisticated light sources have been used, including acousto-optically modulated dye lasers (Thomas et al., 1982); injection-current-modulated edge-emitting diode lasers (Hemmer et al., 1993; Levi et al., 1997); phase-locked external cavity diode lasers (ECDLs) (Brandt et al., 1997; Zanon et al., 2005) or edge-emitting lasers (Zhu & Cutler, 2000); injection-current-modulated vertical-cavity surface-emitting lasers (VCSELs) (Affolderbach et al., 2000; Braun et al., 2007; DeNatale et al., 2008; Kitching et al., 2000; Lutwak et al., 2003; Serkland et al., 2007; Youngner et al., 2007); and electro-optically modulated ECDLs (Jau et al., 2004a). Each of these light sources has relative merits and detriments. For example, VCSELs have very low threshold currents, making them ideal for low-power instruments based on CPT, but suffer from inflexibility with respect to the modulation sideband spectrum. The spectrum of phase-locked ECDLs can be controlled

very precisely, but the locking is
Acousto- and electro-optically m
amplitude modulation with no
large, cumbersome, and expensi

Novel lasers, developed for C
extended cavity (Gavra et al., 20
with a low-reflectivity coating c
These lasers were developed to ha
the need for even a modest amou
10 μW of optical power is sufficie

4.4 Dark Resonances in Thin C

Considerable recent work has fo
atoms confined in cells for which
the transit time across the cell is s
(Briaudeau et al., 1996). In these
cular to the cell walls do not b
before the wall-induced relaxati
the optical absorption. By contra
the cell walls do not collide wit
build up coherence and exhibit
work in this area has focused o
that are observed in these media
Petrosyan & Malakyan, 2000; Sa
widths are typically very large
proceeding to evaluate how the
atomic clocks (Lenci et al., 2009).

4.5 The Lineshape of CPT Reso

The simplest theories of the CP
collisional or diffusion-induced
tion. These relaxation mechanis
width found for most spectrosco
of physical effects that occur in r
resonance lineshape. It has been
intensity distribution of the excit
beam diameter is smaller than th
ground-state relaxation time sca
near its center can result (Levi
2005a) to form a pointed resonan
explained by diffusion-induced
on the Ramsey effect, in which

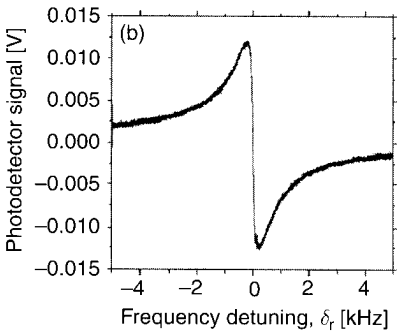

ce-induced resonances for phase-shifted, ed, conventional CPT resonance, (b) both otodetectors subtracted. Reprinted figure 06); © 2006 of the Optical Society of America

opulation Trapping

ces have been used to generate the to excite hyperfine CPT resonances. nts of the light source are not nearly opy, the lamps currently used in con- be too incoherent to generate CPT ast. The requirement on the coherence the light source be smaller than the sitions in the alkali atoms, typically gahertz to several tens of gigahertz. t, which allows great latitude in laser respect to other criteria.

T were carried out using multimode e then, a variety of more sophisticated ding acousto-optically modulated dye ion-current-modulated edge-emitting evi et al., 1997); phase-locked external dt et al., 1997; Zanon et al., 2005) or r, 2000); injection-current-modulated sers (VCSELs) (Affolderbach et al., al., 2008; Kitching et al., 2000; Lutwak Youngner et al., 2007); and electro- al., 2004a). Each of these light sources For example, VCSELs have very low leal for low-power instruments based with respect to the modulation side- hase-locked ECDLs can be controlled

very precisely, but the locking is difficult to implement experimentally. Acousto- and electro-optically modulated sources can have nearly perfect amplitude modulation with no associated phase modulation, but are large, cumbersome, and expensive.

Novel lasers, developed for CPT experiments, include VCSELs in an extended cavity (Gavra et al., 2008), and very short edge emitting lasers with a low-reflectivity coating on one facet (Kargapoltsev et al., 2009). These lasers were developed to have high modulation bandwidths without the need for even a modest amount of output power (in many experiments 10 μW of optical power is sufficient to excite high-contrast resonances).

4.4 Dark Resonances in Thin Cells

Considerable recent work has focused on the optical properties of alkali atoms confined in cells for which the longitudinal dimension is such that the transit time across the cell is shorter than the optical relaxation period (Briaudeau et al., 1996). In these cells, atoms in velocity classes perpendicular to the cell walls do not build up appreciable optical coherence before the wall-induced relaxation and therefore do not contribute to the optical absorption. By contrast, atoms in velocity classes parallel to the cell walls do not collide with the walls as frequently and hence do build up coherence and exhibit corresponding absorption. Some recent work in this area has focused on the understanding of CPT resonances that are observed in these media (Failache et al., 2007; Fukuda et al., 2005; Petrosyan & Malakyan, 2000; Sargsyan et al., 2006). While the CPT line widths are typically very large (greater than 1 MHz), some work is proceeding to evaluate how these systems might be used in compact atomic clocks (Lenci et al., 2009).

4.5 The Lineshape of CPT Resonances: Narrowing Effects

The simplest theories of the CPT resonance lineshape typically involve collisional or diffusion-induced relaxation processes or radiative relaxation. These relaxation mechanisms result in the typical Lorentzian line width found for most spectroscopic signals. However, there are a number of physical effects that occur in real experiments that can distort the CPT resonance lineshape. It has been found, for example, that if the transverse intensity distribution of the excitation light field is non-uniform, or if the beam diameter is smaller than the diffusion length of the atoms over the ground-state relaxation time scales, then a narrowing of the resonance near its center can result (Levi et al., 2000; Taichenachev et al., 2004a, 2005a) to form a pointed resonance lineshape. This lineshape can also be explained by diffusion-induced narrowing (Xiao et al., 2006, 2008) based on the Ramsey effect, in which atoms diffuse out and then re-enter the

excitation beam before relaxing. Finally, propagation effects are known to cause modifications of the resonance line width compared to that observed in an optically thin medium (Godone et al., 2002d). The optical absorption coefficient is smaller when the CPT resonance condition is satisfied, and because the absorption in an optically dense medium is nonlinear as a function of propagation length, significantly more light may be transmitted when on resonance compared to when away from resonance, producing an artificial narrowing effect. However, it remains unclear whether these unusual lineshapes can be effectively used to improve the performance of a CPT atomic clock in some way.

5. CONCLUSIONS AND OUTLOOK

After considering the many possibilities for improving CPT resonances for use in atomic clocks, it is perhaps important to ask to what extent these techniques have impacted the design and performance of actual devices. To some extent this question is premature, as it often takes considerable time for new knowledge, even if it allows clear performance improvements, to find its way into realized systems implemented in the laboratory or in a commercial setting. The cost, time, and risk associated with implementing a new technique to replace, for example, an already proven commercial instrument or an already-operating laboratory instrument are often considered too high. In addition, until experiments are engineered at a level that their importance emerges, issues believed to be ultimately important, such as the effects of the light shift on the long-term stability of the clock, are often masked by other more technical effects, such as temperature-induced shifts. It is therefore often difficult to establish a clear measure of the improvements certain techniques will allow [see, for example, the work by Shah et al. (2006a)].

However, CPT as a whole has now been not just successful for laboratory instruments, but appears to be on the verge of commercial success (DeNatale et al., 2008; Deng, 2008; Lutwak et al., 2007; Vanier et al., 2005; Youngner et al., 2007). In particular, CPT has been shown to be the method of choice for microfabricated vapor cell frequency standards. This is interesting because comparisons of CPT techniques to conventional OMDR techniques for vapor cell frequency references (Kitching et al., 2002; Lutwak et al., 2002; Vanier, 2001b, 2005) have suggested that there is no clear advantage to be gained through the use of CPT with respect to short-term stability. From a technical viewpoint, the biggest strengths of the CPT approach at present therefore appear to be that (a) the physics package design is simple to implement, and (b) that the considerable work over the last 10 years on miniaturized CPT frequency references has clearly established the technical viability of this approach.

While it remains possible that
based on OMDR will ultimatel
parts, considerable work is n
further for miniaturized devi
looked, advantage of CPT is t
of modulation at a subharmoni
the LO to be placed in close p
having radiated RF power inte

Probably the most importa
described above has been the
to excite the resonances. The
availability of commercial diod
The improvements gained by
motivated the development of
use of the D1 line is clearly
stability and (b) that there is no
Certain other design improvem
contrast, such as the end-reson
ing, and the linear polarization
in principle, but work is needed
real clock experiment. The addi
ing impact on reliability will al
which these techniques will be
ques to reduce the light shift, su
engineering, are expected to be
clocks, for which the enginee
technical limitations to the long

Whatever the outcome from
that the understanding of CPT a
considerably over the last deca

ACKNOWLEDGMENTS

We gratefully acknowledge v
A. Post. This work is a partial
Government, and is not subject

REFERENCES

Affolderbach, C., Mileti, G., Andreeva,
May 4–8). Reducing light-shift eff
standards. Proceedings of the Joint
Symposium & PDA Exhibition and
FL, 27–30.

ally, propagation effects are known to
ance line width compared to that
m (Godone et al., 2002d). The optical
hen the CPT resonance condition is
on in an optically dense medium is
tion length, significantly more light
ance compared to when away from
arrowing effect. However, it remains
neshapes can be effectively used to
atomic clock in some way.

LOOK

ilities for improving CPT resonances
aps important to ask to what extent
e design and performance of actual
tion is premature, as it often takes
ge, even if it allows clear performance
realized systems implemented in the
g. The cost, time, and risk associated
e to replace, for example, an already
already-operating laboratory instru-
n. In addition, until experiments are
rtance emerges, issues believed to be
ects of the light shift on the long-term
ked by other more technical effects,
It is therefore often difficult to estab-
ements certain techniques will allow
et al. (2006a)].
w been not just successful for labora-
on the verge of commercial success
utwak et al., 2007; Vanier et al., 2005;
ar, CPT has been shown to be the
ted vapor cell frequency standards.
isons of CPT techniques to conven-
cell frequency references (Kitching
ier, 2001b, 2005) have suggested that
gained through the use of CPT with
n a technical viewpoint, the biggest
present therefore appear to be that
mple to implement, and (b) that the
ears on miniaturized CPT frequency
e technical viability of this approach.

While it remains possible that highly miniaturized frequency references based on OMDR will ultimately be competitive with their CPT counterparts, considerable work is needed to develop the OMDR approach further for miniaturized devices. One additional, and perhaps overlooked, advantage of CPT is that the resonances can be excited by use of modulation at a subharmonic of the hyperfine frequency. This allows the LO to be placed in close proximity to the physics package without having radiated RF power interfere with the atomic transition.

Probably the most important improvement among the techniques described above has been the use of the D1 line rather than the D2 line to excite the resonances. The D2 line was used initially because of the availability of commercial diode lasers at the 852 nm D2 transition of Cs. The improvements gained by using the D1 line have, to some extent, motivated the development of new lasers, and it now appears that (a) the use of the D1 line is clearly superior with respect to the short-term stability and (b) that there is no significant disadvantage to this approach. Certain other design improvements focused on improving the resonance contrast, such as the end-resonance technique, push–pull optical pumping, and the linear polarization techniques, continue to appear promising in principle, but work is needed to quantify the level of improvement in a real clock experiment. The additional system complexity and corresponding impact on reliability will also be a factor in determining the extent to which these techniques will be used in real-world instruments. Techniques to reduce the light shift, such as pulsed CPT and sideband spectrum engineering, are expected to be important for future generations of CPT clocks, for which the engineering has progressed to the point where technical limitations to the long-term instability have been suppressed.

Whatever the outcome from an instrumentation perspective, it is clear that the understanding of CPT as it applies to atomic clocks has advanced considerably over the last decade.

ACKNOWLEDGMENTS

We gratefully acknowledge valuable comments from S. Knappe and A. Post. This work is a partial contribution of NIST, an agency of the US Government, and is not subject to copyright.

REFERENCES

Affolderbach, C., Mileti, G., Andreeva, C., Slavov, D., Karaulanov, T., & Cartaleva, S. (2003, May 4–8). Reducing light-shift effects in optically-pumped gas-cell atomic frequency standards. Proceedings of the Joint Meeting 2003 IEEE International Frequency Control Symposium & PDA Exhibition and 17th European Frequency and Time Forum, Tampa, FL, 27–30.

Affolderbach, C., Nagel, A., Knappe, S., Jung, C., Wiedenmann, D., & Wynands, R. (2000). Nonlinear spectroscopy with a vertical-cavity surface-emitting laser (VCSEL). *Applied Physics B, 70*(3), 407–413.

Akatsuka, T., Takamoto, M., & Katori, H. (2008). Optical lattice clocks with non-interacting bosons and fermions. *Nature Physics, 4*(12), 954–959.

Akulshin, A. M., & Ohtsu, M. (1994). Pulling of the emission frequency of an injection laser by Doppler-free absorption resonances in an intracavity cell. *Quantum Electronics, 24*(7), 561–562.

Allan, D. W. (1966). Statistics of atomic frequency standards. *Proceedings of the IEEE, 54*(2), 221–230.

Alzetta, G., Gozzini, A., Moi, L., & Orriols, G. (1976). Experimental-method for observation of Rf transitions and laser beat resonances in oriented Na vapor. *Il Nuovo Cimento, 36*(1), 5–20.

Arditi, M. (1958, May 6–8)., Gas cell "atomic clocks" using buffer gases and optical orientation. Proceedings of the 12th Annual Symposium on Frequency Control, Fort Monmouth, NJ. Piscataway, NJ: IEEE, 606–622.

Arditi, M., & Carver, T. R. (1961). Pressure, light and temperature shifts in optical detection of 0-0 hyperfine resonances in alkali metals. *Physical Review, 124*(3), 800–809.

Arimondo, E. (1996). Coherent population trapping in laser spectroscopy. *Progress in Optics, 35*, 257–354.

Arimondo, E., & Orriols, G. (1976). Non-absorbing atomic coherences by coherent 2-photon transitions in a 3-level optical-pumping. *Lettere Al Nuovo Cimento, 17*(10), 333–338.

Aspect, A., Arimondo, E., Kaiser, R., Vansteenkiste, N., & Cohentannoudji, C. (1988). Laser cooling below the one-photon recoil energy by velocity-selective coherent population trapping. *Physical Review Letters,* 61(7), 826–829.

Barnes, J. A., Chi, A. R., Cutler, L. S., Healey, D. J., Leeson, D. B., Mcgunical, T. F., et al. (1971). Characterization of frequency stability. *IEEE Transactions on Instrumentation and Measurement, 20*(2), 105–120.

Bell, W. E., & Bloom, A. L. (1961). Optically driven spin precession. *Physical Review Letters, 6*, 280–283.

Boudot, R., Guerandel, S., De Clercq, E., Dimarcq, N., & Clairon, A. (2009). Current status of a pulsed CPT Cs cell clock. *IEEE Transactions on Instrumentation and Measurement, 58*(4), 1217–1222.

Brandt, S., Nagel, A., Wynands, R., & Meschede, D. (1997). Buffer-gas-induced linewidth reduction of coherent dark resonances to below 50 Hz. *Physical Review A, 56*(2), R1063–R1066.

Braun, A. M., Davis, T. J., Kwakernaak, M. H., Michalchuk, J. J., Ulmer, A., Chan, W. K., et al. (2007, November 26–29). RF-interrogated end-state chip-scale atomic clock. Proceedings of the 39th Annual Precise Time and Time Interval (PTTI) Meeting, Long Beach, CA, 233–248.

Briaudeau, S., Bloch, D., & Ducloy, M. (1996). Detection of slow atoms in laser spectroscopy of a thin vapor film. *Europhysics Letters, 35*(5), 337–342.

Camparo, J. C., & Coffer, J. G. (1999). Conversion of laser phase noise to amplitude noise in a resonant atomic vapor: The role of laser linewidth. *Physical Review A, 59*(1), 728–735.

Carver, T. R. (1957, May 7–9). Rubidium oscillator experiments. Proceedings of the 11th Annual Symposium on Frequency Control, Fort Monmouth, NJ. Piscataway, NJ: IEEE, 307–317., May 7–9).

Castagna, N., Boudot, R., Guerandel, S., Clercq, E., Dimarcq, N., & Clairon, A. (2009). Investigations on continuous and pulsed interrogation for a CPT atomic clock. *IEEE Transactions on Ultrasonics, Ferroelectrics and Frequency Control, 56*(2), 246–253.

Castagna, N., Guerandel, S., Dahes, F., Zanon, T., De Clercq, E., Clairon, A., et al. (2007). Frequency stability measurement of a Raman-Ramsey Cs clock. 2007 IEEE International Frequency Control Symposium and the 21st European Frequency and Time Forum, 67–70.

Clairon, A., Salomon, C., Guellati, S., & Phillips, W. D. (1991). Ramsey resonance in a Zacharias fountain. *Europhysics Letters, 16*(2), 165–170.

Cohen-Tannoudji, C., Dupont-Roc, J., & York: Wiley.

Cyr, N., Tetu, M., & Breton, M. (1993 proposal. *IEEE Transactions on Instru*

Delany, M., Bonnette, K.N., & Janssen, Trademark Office.

Denatale, J. F., Borwick, R. L., Tsai, C., St 6–8). Compact, low-power chip-scal Location and Navigation Symposium

Deng, J. (2001). US Patent # 6,172,570. U

Deng, J. (2008, April 22–25). A commer European Frequency and Time Forur

Dicke, R. H. (1953). The effect of collision *Review, 89*(2), 472–473.

Essen, L., & Parry, V. I. (1955). An atomi *176*, 280–284.

Ezekiel, S., Hemmer, P. R., & Leiby, C. stimulated, resonance Raman transi *Review Letters, 50*(7), 549–549.

Failache, H., Lenci, L., & Lezama, A. (20 metric thin cells. *Physical Review A, 7*

Farkas, D.M., Zozulya, A., & Anderson clock based on ultracold trapped Rb

Fukuda, K., Toriyama, A., Izmailov, A. Cs atoms velocity-selected in a thin 503–509.

Gavra, N., Ruseva, V., & Rosenbluh, M efficiency of vertical cavity surface-e *Letters, 92*(22), 221113.

Gerginov, V., Knappe, S., Shah, V., Hollber in single-cell CPT clocks. *IEEE Trans* 1357–1361.

Godone, A., Levi, F., & Micalizio, S. (2002 population-trapping maser. *Physical R*

Godone, A., Levi, F., & Micalizio, S. (2002 population trapping maser. *Physical R*

Godone, A., Levi, F., & Micalizio, S. (20 coherent-population-trapping Rb mas

Godone, A., Levi, F., Micalizio, S., & Va trapping maser: A strong-field self-co

Godone, A., Levi, F., Micalizio, S., & Van inversion phenomena and line widt 5–13.

Godone, A., Levi, F., & Vanier, J. (1999). C inversion: A new atomic frequency s *Measurement, 48*(2), 504–507.

Godone, A., Micalizio, S., Calosso, C. E., & *Transactions on Ultrasonics Ferroelectrics*

Godone, A., Micalizio, S., & Levi, F. (200 *Physical Review A, 70*(2), 023409.

Godone, A., Micalizio, S., Levi, F., & C frequency stability of the pulsed rubid

Goldenberg, H., Kleppner, D., & Ramsey, with stored beams. *Physical Review, 12*

Gordon, J. P., Zeiger, H. J., & Townes, C new hyperfine structure in the micro 282–284.

Cohen-Tannoudji, C., Dupont-Roc, J., & Grynberg, G. (1992). *Atom-photon interactions*. New York: Wiley.

Cyr, N., Tetu, M., & Breton, M. (1993). All-optical microwave frequency standard - a proposal. *IEEE Transactions on Instrumentation and Measurement, 42*(2), 640–649.

Delany, M., Bonnette, K.N., & Janssen, D. (2001). US Patent # 6,265,945. US Patent and Trademark Office.

Denatale, J. F., Borwick, R. L., Tsai, C., Stupar, P. A., Lin, Y., Newgard, R. A., et al. (2008, May 6–8). Compact, low-power chip-scale atomic clock. Proceedings of the IEEE Position Location and Navigation Symposium (PLANS), Monterey, CA, 67–70.

Deng, J. (2001). US Patent # 6,172,570. US Patent and Trademark Office.

Deng, J. (2008, April 22–25). A commercial CPT Rubidium clock. Proceedings of the 2008 European Frequency and Time Forum, Toulouse, France. Session 3b.

Dicke, R. H. (1953). The effect of collisions upon the Doppler width of spectral lines. *Physical Review, 89*(2), 472–473.

Essen, L., & Parry, V. I. (1955). An atomic standard of frequency and time interval. *Nature, 176*, 280–284.

Ezekiel, S., Hemmer, P. R., & Leiby, C. C. (1983). Observation of Ramsey fringes using a stimulated, resonance Raman transition in a sodium atomic-beam - reply. *Physical Review Letters, 50*(7), 549–549.

Failache, H., Lenci, L., & Lezama, A. (2007). Theoretical study of dark resonances in micrometric thin cells. *Physical Review A, 76*(5), 053826.

Farkas, D.M., Zozulya, A., & Anderson, D.Z. (2009). A compact microchip-based atomic clock based on ultracold trapped Rb atoms. arXiv:0912.4231v1 [physics.atom-ph].

Fukuda, K., Toriyama, A., Izmailov, A. C., & Tachikawa, M. (2005). Dark resonance of Cs atoms velocity-selected in a thin cell. *Applied Physics B-Lasers and Optics, 80*(4–5), 503–509.

Gavra, N., Ruseva, V., & Rosenbluh, M. (2008). Enhancement in microwave modulation efficiency of vertical cavity surface-emitting laser by optical feedback. *Applied Physics Letters, 92*(22), 221113.

Gerginov, V., Knappe, S., Shah, V., Hollberg, L., & Kitching, J. (2008). Laser noise cancellation in single-cell CPT clocks. *IEEE Transactions on Instrumentation and Measurement, 57*(7), 1357–1361.

Godone, A., Levi, F., & Micalizio, S. (2002a). Propagation and density effects in the coherent-population-trapping maser. *Physical Review A, 65*(3), 033802.

Godone, A., Levi, F., & Micalizio, S. (2002b). Slow light and superluminality in the coherent population trapping maser. *Physical Review A, 66*(4), 043804.

Godone, A., Levi, F., & Micalizio, S. (2002c). Subcollisional linewidth observation in the coherent-population-trapping Rb maser. *Physical Review A, 65*(3), 031804.

Godone, A., Levi, F., Micalizio, S., & Vanier, J. (2000). Theory of the coherent population trapping maser: A strong-field self-consistent approach. *Physical Review A, 62*(5), 053402.

Godone, A., Levi, F., Micalizio, S., & Vanier, J. (2002d). Dark-line in optically-thick vapors: inversion phenomena and line width narrowing. *European Physical Journal D, 18*(1), 5–13.

Godone, A., Levi, F., & Vanier, J. (1999). Coherent microwave emission without population inversion: A new atomic frequency standard. *IEEE Transactions on Instrumentation and Measurement, 48*(2), 504–507.

Godone, A., Micalizio, S., Calosso, C. E., & Levi, F. (2006a). The pulsed rubidium clock. *IEEE Transactions on Ultrasonics Ferroelectrics and Frequency Control, 53*(3), 525–529.

Godone, A., Micalizio, S., & Levi, F. (2004). Pulsed optically pumped frequency standard. *Physical Review A, 70*(2), 023409.

Godone, A., Micalizio, S., Levi, F., & Calosso, C. (2006b). Physics characterization and frequency stability of the pulsed rubidium maser. *Physical Review A, 74*(4), 043401.

Goldenberg, H., Kleppner, D., & Ramsey, N. F. (1961). Atomic beam resonance experiments with stored beams. *Physical Review, 123*(2), 530–537.

Gordon, J. P., Zeiger, H. J., & Townes, C. H. (1954). Molecular microwave oscillator and new hyperfine structure in the microwave spectrum of NH3. *Physical Review, 95*(1), 282–284.

Gray, H. R., Whitley, R. M., & Stroud, J.C.R. (1978). Coherent trapping of atomic populations. *Optics Letters 3*(6), 218–220.

Guerandel, S., Zanon, T., Castagna, N., Dahes, F., De Clercq, E., Dimarcq, N., et al. (2007). Raman–Ramsey interaction for coherent population trapping Cs clock. *IEEE Transactions on Instrumentation and Measurement, 56*(2), 383–387.

Guo, T., Deng, K., Chen, X. Z., & Wang, Z. (2009). Atomic clock based on transient coherent population trapping. *Applied Physics Letters, 94*(15), 151108.

Happer, W. (1972). Optical pumping. *Reviews of Modern Physics, 44*(2), 169–249.

Hemmer, P. R., Ezekiel, S., & Leiby, J.C.C. (1983a). Stabilization of a microwave-oscillator using a resonance Raman transition in a sodium beam. *Progress in Quantum Electronics, 8* (3–4), 161–163.

Hemmer, P. R., Ezekiel, S., & Leiby, J.C.C. (1983b). Stabilization of a microwave oscillator using a resonance Raman transition in a sodium beam. *Optics Letters, 8*(8), 440–442.

Hemmer, P. R., Ezekiel, S., & Leiby, C. C. (1984). Performance of a microwave clock based on a laser-induced stimulated Raman interaction. *Journal of the Optical Society of America B, 1*(3), 528–528.

Hemmer, P. R., Katz, D. P., Donoghue, J., Croningolomb, M., Shahriar, M. S., & Kumar, P. (1995). Efficient low-intensity optical-phase conjugation based on coherent population trapping in sodium. *Optics Letters, 20*(9), 982–984.

Hemmer, P. R., Ontai, G. P., & Ezekiel, S. (1986). Precision studies of stimulated-resonance Raman interactions in an atomic beam. *Journal of the Optical Society of America B, 3*(2), 219–230.

Hemmer, P. R., Shahriar, M. S., Lamelarivera, H., Smith, S. P., Bernacki, B. E., & Ezekiel, S. (1993). Semiconductor-laser excitation of Ramsey fringes by using a Raman transition in a cesium atomic-beam. *Journal of the Optical Society of America B-Optical Physics, 10*(8), 1326–1329.

Hemmer, P. R., Shahriar, M. S., Natoli, V. D., & Ezekiel, S. (1989). Ac Stark shifts in a two-zone Raman interaction. *Journal of the Optical Society of America B, 6*(8), 1519–1528.

Hong, T., Cramer, C., Nagourney, W., & Fortson, E. N. (2005). Optical clocks based on ultranarrow three-photon resonances in alkaline earth atoms. *Physical Review Letters, 94*(5), 050801.

Jau, Y. Y., & Happer, W. (2005). Simultaneous stabilization of frequency and magnetic field with the tilted 0-0 state. *Applied Physics Letters, 87*(20), 204108.

Jau, Y. Y., & Happer, W. (2007). Push-pull laser-atomic oscillator. *Physical Review Letters, 99,* 223001.

Jau, Y. Y., Miron, E., Post, A. B., Kuzma, N. N., & Happer, W. (2004a). Push-pull optical pumping of pure superposition states. *Physical Review Letters, 93*(16), 160802.

Jau, Y. Y., Post, A. B., Kuzma, N. N., Braun, A. M., Romalis, M. V., & Happer, W. (2004b). Intense, narrow atomic-clock resonances. *Physical Review Letters, 92*(11), 110801.

Kargapoltsev, S. V., Kitching, J., Hollberg, L., Taichenachev, A. V., Velichansky, V. L., & Yudin, V. I. (2004). High-contrast dark resonance in sigma(+)-sigma(-) optical field. *Laser Physics Letters, 1*(10), 495–499.

Kargapoltsev, S. V., Velichansky, V. L., Vasilev, V. V., Kobyakoya, M. S., Morozyuk, A. V., & Shiryaeva, N. V. (2009). Low-threshold short-cavity diode laser for a miniature atomic clock. *Quantum Electronics, 39*(6), 487–493.

Kasevich, M. A., Riis, E., Chu, S., & Devoe, R. G. (1989). Rf spectroscopy in an atomic fountain. *Physical Review Letters, 63*(6), 612–616.

Kastler, A. (1963). Displacement of energy levels of atoms by light. *Journal of the Optical Society of America, 53*(8), 902–906.

Kazakov, G., Matisov, B., Mazets, I., Mileti, G., & Delporte, J. (2005a). Pseudoresonance mechanism of all-optical frequency-standard operation. *Physical Review A, 72*(6), 063408.

Kazakov, G., Mazets, I., Rozhdestvensky, Y., Mileti, G., Delporte, J., & Matisov, B. (2005b). High-contrast dark resonance on the D-2-line of Rb-87 in a vapor cell with different directions of the pump-probe waves. *European Physical Journal D, 35*(3), 445–448.

Kelley, P. L., Harshman, P. J., Blum, O., & Gustafson, T. K. (1994). Radiative renormalization analysis of optical double resonance. *Journal of the Optical Society of America B, 11*(11), 2298–2302.

Kitching, J., Hollberg, L., Knappe, S.,
on coherent population trapping.
Kitching, J., Knappe, S., & Hollberg,
ences. *Applied Physics Letters, 81*(3
Kitching, J., Knappe, S., Vukicevic, N.
microwave frequency reference
vapor. *IEEE Transactions on Instru*
Kitching, J.E., Robinson, H.G., Hollbe
9–14). Compact microwave freque
Proceedings of the 6th Symposium
Scotland. Singapore: World Scient
Knappe, S. (2001). Dark resonance m
ment of Physics, University of Bo
Knappe, S. (2007). MEMS atomic cloc
Comprehensive microsystem. (pp. 57
Knappe, S., Kitching, J., Hollberg, L.
coherent population trapping reso
Knappe, S., Shah, V., Schwindt, P.D.D
microfabricated atomic clock. *App*
Knappe, S., Wynands, R., Kitching, J.
tion of coherent population-trappi
of the Optical Society of America B,
Lenci, L., Lezama, A., & Failache, H.
atomic-frequency references. *Optic*
Levi, F., Calosso, C., Micalizio, S., Goo
5–7). CPT maser clock evaluation
quency and Time Forum, Guildfo
Levi, F., Godone, A., Novero, C., &
hyperfine frequency excitation in
Annual European Frequency and
Levi, F., Godone, A., Vanier, J., Micali
and maser emission profile in CP
Liu, Z. D., Juncar, P., Bloch, D., & Duc
schemes for all-optical microwav
2318–2320.
Lounis, B., & Cohen-Tannoudji, C. (19
Journal De Physique II, 2(4), 579–59
Lutwak, R., Emmons, D., English, T
December 2–4).The chip-scale ato
of the 35th Annual Precise Time
467–478.
Lutwak, R., Emmons, D., Riley, W.,
scale atomic clock – coherent pop
ceedings of the 34th Annual Precis
539–550.
Lutwak, R., Rashed, A., Varghese, M.
29–June 1). The miniature atomic c
Joint Meeting of the European Tir
national Frequency Control Symp
NJ: IEEE, 1327–1333.
Merimaa, M., Lindvall, T., Tittonen, I.,
coherent population trapping in R
Physics, 20(2), 273–279.
Mileti, G., Deng, J. Q., Walls, F. L., Jen
rubidium frequency standards: N
Electronics, 34(2), 233–237.
Nagel, A., Affolderbach, C., Knappe,
hyperfine structure on ground-stat

Kitching, J., Hollberg, L., Knappe, S., & Wynands, R. (2001a). Compact atomic clock based on coherent population trapping. *Electronics Letters, 37*(24), 1449–1451.
Kitching, J., Knappe, S., & Hollberg, L. (2002). Miniature vapor-cell atomic-frequency references. *Applied Physics Letters, 81*(3), 553–555.
Kitching, J., Knappe, S., Vukicevic, N., Hollberg, L., Wynands, R., & Weidmann, W. (2000). A microwave frequency reference based on VCSEL-driven dark line resonances in Cs vapor. *IEEE Transactions on Instrumentation and Measurement, 49*(6), 1313–1317.
Kitching, J.E., Robinson, H.G., Hollberg, L.W., Knappe, S., & Wynands, R. (2001b, September 9–14). Compact microwave frequency reference based on coherent population trapping. Proceedings of the 6th Symposium on Frequency Standards and Metrology, St. Andrews, Scotland. Singapore: World Scientific, 167–174.
Knappe, S. (2001). Dark resonance magnetometers and atomic clocks. PhD Thesis, Department of Physics, University of Bonn, Bonn, Germany.
Knappe, S. (2007). MEMS atomic clocks. In Gianchandani, Y., Tabata, O., & Zappe, H., (Eds.) *Comprehensive microsystem.* (pp. 571–612) Maryland Heights, MO: Elsevier B. V.
Knappe, S., Kitching, J., Hollberg, L., & Wynands, R. (2002). Temperature dependence of coherent population trapping resonances. *Applied Physics B, 74*(3), 217–222.
Knappe, S., Shah, V., Schwindt, P.D.D., Hollberg, L., Kitching, J., Liew, L. A., et al. (2004). A microfabricated atomic clock. *Applied Physics Letters, 85*(9), 1460–1462.
Knappe, S., Wynands, R., Kitching, J., Robinson, H. G., & Hollberg, L. (2001). Characterization of coherent population-trapping resonances as atomic frequency references. *Journal of the Optical Society of America B, 18*(11), 1545–1553.
Lenci, L., Lezama, A., & Failache, H. (2009). Dark resonances in thin cells for miniaturized atomic-frequency references. *Optics Letters, 34*(4), 425–427.
Levi, F., Calosso, C., Micalizio, S., Godone, A., Bertacco, E. K., Detoma, E., et al. (2004, April 5–7). CPT maser clock evaluation for Galileo. Proceedings of the 18th European Frequency and Time Forum, Guildford, UK, 233–238.
Levi, F., Godone, A., Novero, C., & Vanier, J. (1997). On the use of a modulated laser for hyperfine frequency excitation in passive frequency standards. Proceedings of the 11th Annual European Frequency and Time Forum, Neuchatel, Switzerland, 216–220.
Levi, F., Godone, A., Vanier, J., Micalizio, S., & Modugno, G. (2000). Line-shape of dark line and maser emission profile in CPT. *European Physical Journal D, 12*(1), 53–59.
Liu, Z. D., Juncar, P., Bloch, D., & Ducloy, M. (1996). Raman polarization-selective feedback schemes for all-optical microwave frequency standards. *Applied Physics Letters, 69*(16), 2318–2320.
Lounis, B., & Cohen-Tannoudji, C. (1992). Coherent population trapping and fano profiles. *Journal De Physique II, 2*(4), 579–592.
Lutwak, R., Emmons, D., English, T., Riley, W., Duwel, A., Varghese, M., et al. (2003, , December 2–4).The chip-scale atomic clock – recent development progress. Proceedings of the 35th Annual Precise Time and Time Interval (PTTI) Meeting, San Diego, CA, 467–478.
Lutwak, R., Emmons, D., Riley, W., & Garvey, R. M. (2002,, December 3–5). The chip-scale atomic clock – coherent population trapping vs. conventional interrogation. Proceedings of the 34th Annual Precise Time and Time Interval (PTTI) Meeting, Reston, VA, 539–550.
Lutwak, R., Rashed, A., Varghese, M., Tepolt, G., Lebanc, J., Mescher, M., et al. (2007, May 29–June 1). The miniature atomic clock – pre-production results. Proceedings of the 2007 Joint Meeting of the European Time and Frequency Forum (EFTF) and the IEEE International Frequency Control Symposium (IEEE-FCS), Geneva, Switzerland. Piscataway, NJ: IEEE, 1327–1333.
Merimaa, M., Lindvall, T., Tittonen, I., & Ikonen, E. (2003). All-optical atomic clock based on coherent population trapping in Rb-85. *Journal of the Optical Society of America B-Optical Physics, 20*(2), 273–279.
Mileti, G., Deng, J. Q., Walls, F. L., Jennings, D. A., & Drullinger, R. E. (1998). Laser-pumped rubidium frequency standards: New analysis and progress. *IEEE Journal of Quantum Electronics, 34*(2), 233–237.
Nagel, A., Affolderbach, C., Knappe, S., & Wynands, R. (2000). Influence of excited-state hyperfine structure on ground-state coherence. *Physical Review A*, 61(1), 012504.

Nagel, A., Brandt, S., Meschede, D., & Wynands, R. (1999). Light shift of coherent population trapping resonances. *Europhysics Letters, 48*(4), 385–389.

Nagel, A., Graf, L., Naumov, A., Mariotti, E., Biancalana, V., Meschede, D., et al. (1998). Experimental realization of coherent dark-state magnetometers. *Europhysics Letters, 44*(1), 31–36.

Novikova, I., Phillips, D. F., Zibrov, A. S., Walsworth, R. L., Taichenachev, A. V., & Yudin, V. I. (2006a). Cancellation of light shifts in an N-resonance clock. *Optics Letters, 31*(5), 622–624.

Novikova, I., Phillips, D. F., Zibrov, A. S., Walsworth, R. L., Taichenachev, A. V., & Yudin, V. I. (2006b). Comparison of Rb-87 N-resonances for D-1 and D-2 transitions. *Optics Letters, 31*(15), 2353–2355.

Orriols, G. (1979). Non-absorption resonances by non-linear coherent effects in a 3-level system. *Il Nuovo Cimento, 53*(1), 1–24.

Petrosyan, D., & Malakyan, Y. P. (2000). Electromagnetically induced transparency in a thin vapor film. *Physical Review A*, 61(5), 053820.

Post, A. (2003). Studies of atomic clock resonances in miniature vapor cells. PhD Thesis, Department of Physics, Princeton University, Princeton, NJ.

Post, A., Jau, Y. Y., Kuzma, N. N., Braun, A. M., Lipp, S., Abeles, J. H., et al. (2003, December 2–4). End resonance for atomic clocks. Proceedings of the 35th Annual Precise Time and Time Interval (PTTI) Meeting, Washington, DC, 445–456.

Post, A. B., Jau, Y. Y., Kuzma, N. N., & Happer, W. (2005). Amplitude- versus frequency-modulated pumping light for coherent population trapping resonances at high buffer-gas pressure. *Physical Review A*, 72(3), 033417.

Ramsey, N. F. (1950). A molecular beam resonance method with separated oscillating fields. *Physical Review, 78*(6), 695–699.

Renzoni, F., & Arimondo, E. (1998). Population-loss-induced narrowing of dark resonances. *Physical Review A, 58*(6), 4717–4722.

Robinson, H. G., Ensberg, E. S., & Dehmelt, H. G. (1958). Preservation of a spin state in free atom-inert surface collisions. *Bulletin of the American Physical Society, 3*, 9.

Rosenbluh, M., Shah, V., Knappe, S., & Kitching, J. (2006). Differentially detected coherent population trapping resonances excited by orthogonally polarized laser fields. *Optics Express, 14*(15), 6588–6594.

Santra, R., Arimondo, E., Ido, T., Greene, C. H., & Ye, J. (2005). High-accuracy optical clock via three-level coherence in neutral bosonic Sr-88. *Physical Review Letters, 94*(17), 173002.

Sargsyan, A., Sarkisyan, D., & Papoyan, A. (2006). Dark-line atomic resonances in a sub-micron-thin Rb vapor layer. *Physical Review A, 73*(3), 033803.

Schmidt, O., Wynands, R., Hussein, Z., & Meschede, D. (1996). Steep dispersion and group velocity below c/3000 in coherent population trapping. *Physical Review A, 53*(1), R27–R30.

Schwindt, P.D.D., Knappe, S., Shah, V., Hollberg, L., Kitching, J., Liew, L. A., et al. (2004). Chip-scale atomic magnetometer. *Applied Physics Letters, 85*(26), 6409–6411.

Serkland, D. K., Geib, K. M., Peake, G. M., Lutwak, R., Rashed, A., Varghese, M., et al. (2007). VCSELs for atomic sensors. Society of Photo-Optical Instrumentation Engineers (SPIE), 48406–48406.

Shah, V., Gerginov, V., Schwindt, P.D.D., Knappe, S., Hollberg, L., & Kitching, J. (2006a). Continuous light shift correction in modulated CPT clocks. *Applied Physics Letters, 89*, 151124.

Shah, V., Knappe, S., Hollberg, L., & Kitching, J. (2007). High-contrast coherent population trapping resonances using four-wave mixing in Rb-87. *Optics Letters, 32*(10), 1244–1246.

Shah, V., Knappe, S., Schwindt, P.D.D., Gerginov, V., & Kitching, J. (2006b). A compact phase delay technique for increasing the amplitude of coherent population trapping resonances in open Lambda systems. *Optics Letters, 31*(15), 2335–2337.

Stahler, M., Wynands, R., Knappe, S., Kitching, J., Hollberg, L., Taichenachev, A., et al. (2002). Coherent population trapping resonances in thermal Rb-85 vapor: D-1 versus D-2 line excitation. *Optics Letters, 27*(16), 1472–1474.

Strekalov, D., Aveline, D., Matsko, A., Thompson, R., Yu, N., & Maleki, L. (2003, , December 2–4). Opto-electronic oscillator stabilized by a hyperfine atomic transition. Proceedings of the 35th Annual Precise Time and Time Interval (PTTI) Meeting, 479–488.

Strekalov, D., Savchenkov, A., Matsko, A., optical atomic clock on a chip: progres tional Ultrasonics, Ferroelectrics, and ference, Montreal, PQ. Piscataway, NJ:

Taichenachev, A. V., Tumaikin, A. M., Yudin (2004a). Nonlinear-resonance line shap tribution of a light beam. *Physical Revie*

Taichenachev, A. V., Tumaikin, A. M., Yudin (2005a). Nonlinear-resonance line sha distribution of a light beam (vol A 69, 029903.

Taichenachev, A. V., Yudin, V. I., Velicha Kitching, J., et al. (2004b). High-contrast in the field of counterpropagating wave

Taichenachev, A. V., Yudin, V. I., Velichans possibility of significantly increasing th Rb-87. *JETP Letters, 82*(7), 398–403.

Thomas, J. E., Ezekiel, S., Leiby, C. C., P resolution spectroscopy and frequency regions using optical lasers. *Optics Lette*

Thomas, J. E., Hemmer, P. R., Ezekiel, S., L Observation of Ramsey fringes using sodium atomic-beam. *Physical Review L*

Vanier, J. (2001a). US Patent # 6,320,472. US

Vanier, J. (2001b, September 9–14). Coher pumping: On their use in atomic frequ sium on Frequency Standards and Metr Scientific, 155–166., September 9–14).

Vanier, J. (2005). Atomic clocks based on c *Physics B, 81*(4), 421–442.

Vanier, J., & Audoin, C. (1992). *The quant* Adam Hilger.

Vanier, J., Godone, A., & Levi, F. (1998). Coh and coherent microwave emission. *Phys*

Vanier, J., Godone, A., Levi, F., & Micalizi coherent population trapping: Basic theo ings of the Joint Meeting 2003 IEEE Inter Exhibition and 17th European Frequenc

Vanier, J., Levine, M., Kendig, S., Janssen, 23–27).Practical realization of a pass standard. Proceedings of the 2004 IEE Frequency Control 50th Anniversary Joi

Vanier, J., Levine, M. W., Janssen, D., & Del coherent population trapping transmiss optical pumping. *Physical Review A, 67*(6

Vanier, J., Levine, M. W., Janssen, D., & D trapping passive frequency standard. *IE ment, 52*(2), 258–262.

Vanier, J., Levine, M. W., Janssen, D., & D optical pumping and coherent populatio atomic frequency standards. *IEEE Trans* 822–831.

Vanier, J., Levine, M. W., Kendig, S., Jans Practical realization of a passive cohe *IEEE Transactions on Instrumentation and*

Vukicevic, N., Zibrov, A. S., Hollberg, L., W Compact diode-laser based rubidium f *sonics Ferroelectrics and Frequency Control*

Strekalov, D., Savchenkov, A., Matsko, A., Yu, N., & Maleki, L. (2004, August 23–27). All-optical atomic clock on a chip: progress report. Proceedings of the 2004 IEEE International Ultrasonics, Ferroelectrics, and Frequency Control 50th Anniversary Joint Conference, Montreal, PQ. Piscataway, NJ: IEEE, 104–108.

Taichenachev, A. V., Tumaikin, A. M., Yudin, V. I., Stahler, M., Wynands, R., Kitching, J., et al. (2004a). Nonlinear-resonance line shapes: Dependence on the transverse intensity distribution of a light beam. *Physical Review A, 69*(2), 024501.

Taichenachev, A. V., Tumaikin, A. M., Yudin, V. I., Stahler, M., Wynands, R., Kitching, J., et al. (2005a). Nonlinear-resonance line shapes: Dependence on the transverse intensity distribution of a light beam (vol A 69, art non 024501, 2004). *Physical Review A, 71*(2), 029903.

Taichenachev, A. V., Yudin, V. I., Velichansky, V. L., Kargapoltsev, S. V., Wynands, R., Kitching, J., et al. (2004b). High-contrast dark resonances on the D-1 line of alkali metals in the field of counterpropagating waves. *JETP Letters, 80*(4), 236–240.

Taichenachev, A. V., Yudin, V. I., Velichansky, V. L., & Zibrov, S. A. (2005b). On the unique possibility of significantly increasing the contrast of dark resonances on the D1 line of Rb-87. *JETP Letters, 82*(7), 398–403.

Thomas, J. E., Ezekiel, S., Leiby, C. C., Picard, R. H., & Willis, C. R. (1981). Ultrahigh-resolution spectroscopy and frequency standards in the microwave and far-infrared regions using optical lasers. *Optics Letters, 6*(6), 298–300.

Thomas, J. E., Hemmer, P. R., Ezekiel, S., Leiby, C. C., Picard, R. H., & Willis, C. R. (1982). Observation of Ramsey fringes using a stimulated, resonance Raman transition in a sodium atomic-beam. *Physical Review Letters, 48*(13), 867–870.

Vanier, J. (2001a). US Patent # 6,320,472. US Patent and Trademark Office.

Vanier, J. (2001b, September 9–14). Coherent population trapping and intensity optical pumping: On their use in atomic frequency standards. Proceedings of the 6th Symposium on Frequency Standards and Metrology, St. Andrews, Scotland. Singapore: World Scientific, 155–166., September 9–14).

Vanier, J. (2005). Atomic clocks based on coherent population trapping: A review. *Applied Physics B, 81*(4), 421–442.

Vanier, J., & Audoin, C. (1992). *The quantum physics of atomic frequency standards*. Bristol: Adam Hilger.

Vanier, J., Godone, A., & Levi, F. (1998). Coherent population trapping in cesium: Dark lines and coherent microwave emission. *Physical Review A, 58*(3), 2345–2358.

Vanier, J., Godone, A., Levi, F., & Micalizio, S. (2003a, May 4–8). Atomic clocks based on coherent population trapping: Basic theoretical models and frequency stability. Proceedings of the Joint Meeting 2003 IEEE International Frequency Control Symposium & PDA Exhibition and 17th European Frequency and Time Forum, Tampa, FL, 2–15.

Vanier, J., Levine, M., Kendig, S., Janssen, D., Everson, C., & Delany, M. (2004, August 23–27).Practical realization of a passive coherent population trapping frequency standard. Proceedings of the 2004 IEEE International Ultrasonics, Ferroelectrics, and Frequency Control 50th Anniversary Joint Conference, IEEE, Piscataway, NJ, 92–99.

Vanier, J., Levine, M. W., Janssen, D., & Delaney, M. (2003b). Contrast and linewidth of the coherent population trapping transmission hyperfine resonance line in Rb-87: Effect of optical pumping. *Physical Review A, 67*(6), 065801.

Vanier, J., Levine, M. W., Janssen, D., & Delaney, M. J. (2003c). The coherent population trapping passive frequency standard. *IEEE Transactions on Instrumentation and Measurement, 52*(2), 258–262.

Vanier, J., Levine, M. W., Janssen, D., & Delaney, M. J. (2003d). On the use of intensity optical pumping and coherent population trapping techniques in the implementation of atomic frequency standards. *IEEE Transactions on Instrumentation and Measurement, 52*(3), 822–831.

Vanier, J., Levine, M. W., Kendig, S., Janssen, D., Everson, C., & Delaney, M. J. (2005). Practical realization of a passive coherent population trapping frequency standard. *IEEE Transactions on Instrumentation and Measurement, 54*(6), 2531–2539.

Vukicevic, N., Zibrov, A. S., Hollberg, L., Walls, F. L., Kitching, J., & Robinson, H. G. (2000). Compact diode-laser based rubidium frequency reference. *IEEE Transactions on Ultrasonics Ferroelectrics and Frequency Control, 47*(5), 1122–1126.

Walter, D. K., & Happer, W. (2002). Spin-exchange broadening of atomic clock resonances. *Laser Physics, 12*(8), 1182–1187.
Watabe, K., Ikegami, T., Takamizawa, A., Yanagimachi, S., Ohshima, S., & Knappe, S. (2009). High-contrast dark resonances with linearly polarized light on the D-1 line of alkali atoms with large nuclear spin. *Applied Optics, 48*(6), 1098–1103.
Whitley, R. M., & Stroud, C. R. (1976). Double optical resonance. *Physical Review A, 14*(4), 1498–1513.
Wynands, R., & Nagel, A. (1999). Precision spectroscopy with coherent dark states. *Applied Physics B, 68*(1), 1–25.
Xiao, Y., Novikova, I., Phillips, D. F., & Walsworth, R. L. (2006). Diffusion-induced Ramsey narrowing. *Physical Review Letters, 96*, 043601.
Xiao, Y., Novikova, I., Phillips, D. F., & Walsworth, R. L. (2008). Repeated interaction model for diffusion-induced Ramsey narrowing. *Optics Express, 16*(18), 14128–14141.
Yariv, A. (1997). *Optical electronics in modern communications*. Oxford, UK: Oxford University Press.
Yoon, T. H. (2007). Wave-function analysis of dynamic cancellation of ac Stark shifts in optical lattice clocks by use of pulsed Raman and electromagnetically-induced-transparency techniques. *Physical Review A, 76*(1), 013422.
Youngner, D. W., Lust, L. M., Carlson, D. R., Lu, S. T., Forner, L. J., Chanhvongsak, H. M., et al. (2007, June 10–14). A manufacturable chip-scale atomic clock. Proceedings of the IEEE Transducers '07 & Eurosensors XXI Conference, Lyon, France, 39–44.
Zacharias, J.R. (1953). Unpublished. Described in N. F. Ramsey, *Molecular beams* (pp. 138). Oxford, UK: Oxford University Press, 1956.
Zanon, T., Guerandel, S., De Clercq, E., Dimarcq, N., & Clairon, A. (2003, May 4–8). Coherent population trapping with cold atoms. Proceedings of the Joint Meeting 2003 IEEE International Frequency Control Symposium & PDA Exhibition and 17th European Frequency and Time Forum, Tampa, FL, 49–54.
Zanon, T., Guerandel, S., De Clercq, E., Holleville, D., Dimarcq, N., & Clairon, A. (2004a). Coherent population trapping on cold atoms. *Journal de Physique IV, 119*, 291–292.
Zanon, T., Guerandel, S., De Clercq, E., Holleville, D., Dimarcq, N., & Clairon, A. (2005). High contrast Ramsey fringes with coherent-population-trapping pulses in a double lambda atomic system. *Physical Review Letters, 94*(19), 193002.
Zanon, T., Guerandel, S., De Clercq, E., Hollville, D., & Dimarcq, N. (2004b, April 5–7). Observation of Ramsey fringes with optical CPT pulses. Proceedings of the 18th European Frequency and Time Forum, Guildford, UK. Session 1B.
Zanon-Willette, T., Ludlow, A. D., Blatt, S., Boyd, M. M., Arimondo, E., & Ye, J. (2006). Cancellation of stark shifts in optical lattice clocks by use of pulsed Raman and electromagnetically induced transparency techniques. *Physical Review Letters, 97*(23), 233001.
Zhu, M. (2002). US Patent # 6,359,916. US Patent and Trademark Office.
Zhu, M. (2003, May 4–8). High contrast signal in a coherent population trapping based atomic frequency standard application. Proceedings of the Joint Meeting 2003 IEEE International Frequency Control Symposium & PDA Exhibition and 17th European Frequency and Time Forum, Tampa, FL, 16–21.
Zhu, M., & Cutler, L. S. (2000, November 28–30). Theoretical and experimental study of light shift in a CPT-based Rb vapor cell frequency standard. Proceedings of the 32nd Annual Precise Time and Time Interval (PTTI) Meeting, Reston, VA, 311–324.
Zibrov, A. S., Ye, C. Y., Rostovtsev, Y. V., Matsko, A. B., & Scully, M. O. (2002). Observation of a three-photon electromagnetically induced transparency in hot atomic vapor. *Physical Review A, 65*(4), 043817.
Zibrov, S., Novikova, I., Phillips, D. F., Taichenachev, A. V., Yudin, V. I., Walsworth, R. L., et al. (2005). Three-photon-absorption resonance for all-optical atomic clocks. *Physical Review A, 72*(1), 011801.

CHAPTER 3

Dissocia of H_3^+ Io Theory a

Rainer Johns

[a]*Department of Ph Pittsburgh, PA 16*
[b]*Institute for Scien MA 01890, USA*

Contents

1. Introductio
2. Basic Defi
3. Experimen
   3.1 Afterg
   3.2 Single Ring E
4. Theory
   4.1 DR M
   4.2 H_3^+ P
   4.3 Vibrat
   4.4 One-
   4.5 Three
5. History of Studies
6. Reconciling
   6.1 Afterg Very L
   6.2 Afterg High F
   6.3 Third-
7. Comparison
8. H_3^+ Produc
9. Isotope Eff
10. Conclusion
Acknowledgment
References

Advances in Atomic, Molecular, and Optical Phy
ISSN 1049-250X, DOI: 10.1016/S1049-250X(10)59